General Disclaimer

One or more of the Following Statements may affect this Document

- This document has been reproduced from the best copy furnished by the organizational source. It is being released in the interest of making available as much information as possible.

- This document may contain data, which exceeds the sheet parameters. It was furnished in this condition by the organizational source and is the best copy available.

- This document may contain tone-on-tone or color graphs, charts and/or pictures, which have been reproduced in black and white.

- This document is paginated as submitted by the original source.

- Portions of this document are not fully legible due to the historical nature of some of the material. However, it is the best reproduction available from the original submission.

NASA TECHNICAL MEMORANDUM

NASA TM X-72844

NASA TM X-72844

MEASUREMENTS OF AAFE RADSCAT ANTENNA CHARACTERISTICS

by Aubrey E. Cross, W. Linwood Jones, Jr.,

and Alfred L. Jones

June 1977

NATIONAL AERONAUTICS AND SPACE ADMINISTRATION

LANGLEY RESEARCH CENTER, HAMPTON, VIRGINIA 23665

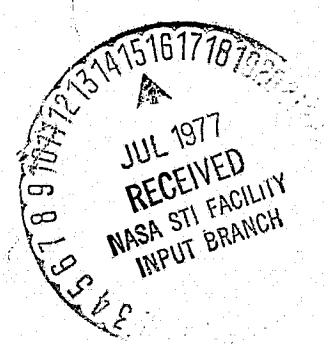

INTRODUCTION

Microwave remote sensing techniques often rely upon an absolute measurement of a microwave observable (received power, phase, doppler frequency, etc.) to infer some physical property of a target. In a few instances, the measurement accuracy is limited by an understanding of the relationship between the microwave and physical observables. A more common cause of measurement uncertainty, however, is instrument error, and frequently this error is the result of the sensor antenna characteristics. The antenna transmits and/or receives electromagnetic radiation in (from) many directions with widely varying efficiency. The output of the receiving antenna is the summation of energy from all directions weighted by the directional efficiency (gain) of the antenna.

For passive (microwave radiometer) measurements, bias errors of several degrees can easily occur for even good quality microwave antennas. Errors of this magnitude are intolerable because they are significant compared to the range of microwave brightness temperature changes with changes in the desired surface property.

For many remote sensing applications, two-dimensional microwave images are required so that the spatial characteristics of the surface parameter can be determined. Again, the antenna radiation pattern can severely mask or distort the measurement. Fortunately, for certain well defined antennas (such as high beam-efficiency pencil-beam types), these distortion effects can be removed by analytical techniques (references 1, 2 and 3). All of these compensating methods, however, require a detailed knowledge of the three dimensional polarized antenna radiation patterns.

Active (radar) measurements also suffer from antenna effects which can be even more complex than those for passive(radiometric) measurements. The radiometer antenna performs an incoherent (scaler) summation of all incident radiation, while the radar receiving antenna performs a coherent (vector) summation of all the electromagnetic field intensities at its aperture. Again the undesirable antenna effects can, in concept, be removed by proper analysis provided the three-dimensional patterns are well known (reference 4).

The purpose of this report is to document the antenna characteristics for the NASA Langley Research Center's Advanced Applications Flight Experiments combined radiometer-scatterometer (AAFE RADSCAT) microwave remote sensor. Tests are described and results presented for both active (radiation patterns) and passive (antenna losses) antenna measurements. These antenna characteristics are required for proper analysis of RADSCAT oceanographic measurements.

EXPERIMENT DESCRIPTION AND RESULTS

Antenna

The AAFE RADSCAT (detailed description in reference 5) has used two different 13.9 GHz pencil beam antennas for ocean measurements. The original was a reproduction of the Skylab S-193 RADSCAT antenna which had a half power (full) beamwidth of approximately 1.5° and a gain of 41. 5 dB. It utilized a parabolic reflector with a diameter of 113 cm (44.5 inches) and an F/D of 0.359, and it had a modified Cuttler feed with dual linear

polarization. In January 1975, this antenna was damaged and was replaced by an antenna using the same feed but a different reflector. This reflector was a parabolic spinning of 0.32 cm ($\frac{1}{8}$ inch) thick aluminum alloy with a 3.2 cm (1-$\frac{1}{4}$ inch) diameter beaded rim for stiffening. It had an effective diameter of 122 cm (48 inches) with an F/D of 0.400. An 18 cm (7 inch) collar fabricated of 0.32 cm ($\frac{1}{8}$ inch) aluminum alloy was welded to the outer edge of the stiffening rim. A photograph of the RADSCAT antenna with a 13.9 GHz feed mounted in the parabolic reflector is shown in figure 1. Although the antenna was designed and equipped with interchangeable feeds for operation at two specific frequencies (9.3 and 13.9 GHz), only the 13.9 GHz feed configuration was used for the pattern measurements.

Antenna Pattern Measurement

Due to RADSCAT instrument commitments, extensive antenna pattern measurements were initially made on the non-certified NASA-LaRC outdoor range to establish reference measurements, and then later, final pattern measurements were made on the certified NASA-JSC range in Houston, Texas. Representative pattern measurements from both ranges are presented following a brief discussion of the LaRC measurement procedure.

Figure 1 shows the NASA-LaRC outdoor range where the RADSCAT antenna can be seen mounted on an azimuth over elevation pedestal. Also shown, to the right background of the pedestal, is the source tower and the transmitting antenna. Figure 2 is a perspective sketch (not to scale) of the antenna range showing the RADSCAT antenna installation. A block diagram of the transmit and receive electronics is shown in figure 3. A standard gain horn was used as the transmitting antenna with a selectable radiation power of either 6 mW or 600 mW. The higher radiation power was used to obtain

detailed measurements of the side lobe and back lobe patterns. During these higher power measurement, the main lobe portion of the patterns are distorted due to saturation of the receiver.

Pattern measurements were made in the two principal planes, E-plane (horizontal polarization) and H-plane (vertical polarization). E-H plane (cross-polarization) patterns were also made. For each fixed polarization condition, the RADSCAT antenna was rotated in azimuth for the pattern measurements. The pattern polarizations are referenced to the orientation of the inline rectangular waveguide that feeds the ortho-mode transducer.

Upon completion of the pattern measurements, the electrical and mechanical boresite of the RADSCAT antenna were checked using the following procedure. Initially, the RADSCAT antenna was electrically alined with the transmitting horn by peaking the received signal gain for both polarizations. This setting was called 0° azimuth and 0° elevation on the positioning pedestal. For mechanical alinement, a laser was then substituted for the transmitting horn and a 10.2 cm (4 inch) diameter plane-parallel mirror was placed normal to the feed point centerline of the RADSCAT antenna as shown in the photograph of figure 4. A sketch of the mechanical boresite alinement method is shown in figure 5. Small azimuth and elevation angle adjustments were then made with the laser (transmitting end) to aline the incident laser beam to intercept the mirror surface. Finally, azimuth and elevation positioning adjustments were made using the RADSCAT antenna pedestal (receiving end). The antenna position was adjusted to cause the reflecting laser beam to coincide with the incident

beam. The result of the final positioning adjustments was the error between the electrical and mechanical boresite. The results are given in table I.

LaRC Patterns.- The LaRC pattern measurements are shown in figures 6 through 19. The measurements are presented in four general groupings for ease of interpretation and for comparison. The general groupings are as follows: pattern modification due to the cylindrical collar, figures 6 through 12; operating frequency effects, figures 8 through 12; cross polarization patterns, figures 13 and 14; and main beam shaping by feed focusing, figures 15 through 19.

A source frequency of 13.9 GHz was used for all the measurements shown except for figures 11, 12 and 15, where a frequency of 14.0 GHz was used. The cylindrical collar was attached to the antenna for all the patterns presented unless noted otherwise. Feeds 1 and 2, for use at 13.9 GHz, were physically indentical and were tested for comparison of electrical characteristics. A 5.08 cm (2.0 inch) feed extension was used for all patterns unless noted otherwise.

JSC Patterns.- In December 1975, RADSCAT antenna patterns were also measured at 13.9 GHz by the NASA Lyndon B. Johnson Space Center (JSC) in Houston, Texas. These patterns were made on a certified range under the jurisdiction of the Antenna Systems Section of the Tracking and Communications Development Division, JSC. The pattern

measurements are shown in figures 20 through 23. Principal plane patterns using an antenna feed extension of 5.08 cm (2.0 inches) and electrically excited by the inline feed port and the side feed port of the orthomode transducer (OMT) are shown in figures 20 and 21. The patterns shown in figures 22 and 23 used a 3.175 cm (1.25 inches) feed extension, and again, the excitation of the inline and side feed ports of the OMT are shown.

The boresite difference between the electrical and mechanical zero was evaluated by the JSC utilizing laser reflections from a plane surface mirror installed in place of the feed assembly. The results of the JSC boresite checks are given in table II. A comparison of tables I and II thus indicate the small differences between electrical and mechanical alinement of the RADSCAT antenna.

Pattern Analysis.- The reduction of RADSCAT measurements to scattering coefficient (reference 5) requires that the antenna gain and equivalent beamwidth be accurately known. To accomplish this, the patterns of figures 10 and 20 were numerically integrated using the following equations:

$$\theta_{eq} = \sqrt{\frac{4}{\pi} \int_0^{2\pi} \int_0^{\pi} P^2 (\theta, \phi) \sin \theta \, d\theta \, d\phi} \qquad (1)$$

where θ_{eq} = equivalent "pencil beam" width

$P(\theta, \phi)$ = normalized power pattern

θ, ϕ = spherical coordinate angles

$$\Omega = \int_0^{2\pi} \int_0^{\pi} P\left(\theta, \phi\right) \sin\theta \, d\theta \, d\phi \qquad (2)$$

where Ω = the antenna beam solid angle

$$\eta_i = \int_0^{2\pi} \int_0^{\theta_i} P\left(\theta, \phi\right) \sin\theta \, d\theta \, d\phi \qquad (3)$$

where η_i = antenna efficiency

θ_i = angle to the first null of the antenna pattern

$$G = \eta_i \frac{4\pi}{\Omega} \qquad (4)$$

where G = antenna gain

The results of these calculations for both RADSCAT antennas are presented in table III.

Antenna Loss Measurements

Antenna losses were measured at 13.9 GHz using the AAFE RADSCAT in the radiometric mode during two series of calibrations; Table Mountain, California, July 1972, and NASA Wallops Flight Center, December 1972. During these tests the RADSCAT and antenna were placed inside of an inverted truncated pyramidal reflector and the antenna pointed to the vertical (figures 24 and 25). The reflector served to move the antenna side-lobes close to the main beam so that the entire antenna pattern viewed a uniform sky temperature. The vertical profile of atmospheric

temperature and water vapor was measured and used to calculate the zenith sky temperature. The radiometer was used to measure the antenna temperature while viewing both the sky and an ambient temperature absorber load supported above the reflector (figure 26). This procedure produced two widely separated antenna brightness temperatures (300°K, absorber and 7°K, sky) which were used to compute the antenna losses from a transmission line model given in figure 27. The equation from this model is

$$T_{ant} = \left[1 - \Gamma_2^2\right]\left[T_b\left(1 - \Gamma_1^2\right)\frac{1}{L} + \left(1 - \frac{1}{L_f}\right)T_f + \left(1 - \frac{1}{L_{omt}}\right)T_{omt}\right.$$

$$\left. + \left(1 - \frac{1}{L_{wg}}\right)T_{wg} + \Gamma_1^2\, T_{rad}\left(\frac{1}{L}\right)^2\right] \qquad (5)$$

where T_{ant} = Antenna temperature (input to radiometer)

Γ_2 = radiometer voltage reflection coefficient

T_b = microwave brightness temperature (input to antenna)

Γ_1 = antenna voltage reflection coefficient

L = total loss between antenna and radiometer

$= L_f + L_{omt} + L_{wg}$

L_f = feed loss

T_f = physical temperature of feed

L_{omt} = orthomode transducer loss

T_{omt} = physical temperature of omt

L_{wg} = waveguide loss

T_{wg} = physical temperature of waveguide

T_{rad} = output microwave temperature (power) of radiometer (to antenna output)

In previous laboratory tests the voltage reflection coefficients and losses of the orthomode transducer and waveguide were measured; therefore equation 5 was solved for the unknown feed loss. The accuracy of the total antenna loss measurements was primarily determined by the absolute radiometer accuracy ($\pm$ 5°K) and was determined to be $\pm$ 0.10 dB. Results of the antenna measurements are summarized in table IV.

CONCLUDING REMARKS

The antenna characteristics for the AAFE RADSCAT have been measured at 13.9 GHz during a series of field measurements. For the reduction of ocean data prior to January 1975, the Skylab S-193 antenna patterns should be used; whereas afterwards the patterns given herein should be used (see table III). As far as antenna losses are concerned, the values given in table IV are correct for both antennas since the same feed, orthomode transducer, and waveguide were used.

REFERENCE LIST

1. Claassen, J. P. and Fung, A. K.: The Recovery of Polarized Apparent Temperature Distribution of Flat Scenes from Antenna Temperature Measurements, IEEE Trans. Ant. and Prop., Vol. AP-22, pp. 433-442, May 1974.

2. Beck, F. B.: Antenna Pattern Corrections to Microwave Radiometer Temperature Calculations, Radio Science, Vol. 10, Number 10, pp. 839-845, October 1975.

3. Truman, W. M.: Three-Dimensional Vector Modeling and Restoration of Flat Finite Wave Tank Radiometric Measurements, Ph. D. Dissertation, Dept. of Elec. Engr., West Virginia University, 1976.

4. Claassen, J. P. and Fung, A. K.: The Recovery of Microwave Scattering Parameters from Scatterometric Measurements with Special Application to the Sea, NASA CR-132748, November 1975.

5. Schroeder, L. C., Jones, W. L. and Mitchell, J. L.: Laboratory Calibration of AAFE Radiometer/Scatterometer (RADSCAT), NASA TMX-73900, November 1976.

TABLE I.- LaRC BORESITE*

Roll Angle	Mechanical Error	
	Az.	El.
0°	0.085°	0.065°
360°	0.030°	0.060°

TABLE II.- JSC BORESITE*

Roll Angle	Mechanical Error	
	Az	El.
0°	-0.36°	0.08°
90°	-0.26°	-0.02°
180°	-0.34°	-0.09°
270°	-0.21°	-0.14°

*Electrical boresite set to zero for azimuth and elevation.

TABLE III.- ANTENNA GAIN AND BEAMWIDTH AT 13.9 GHz

DATES	GAIN, dB	EFFECTIVE BEAMWIDTH, RADIANS
OCT. 72 - DEC. 74	41.5	0.0225
AFTER JAN. 75	41.7	0.0201

TABLE IV.- ANTENNA LOSSES AT 13.9 GHz

	L_{wg}, dB		L_{omt}, dB		L_f, dB		L, dB	
TEST	VERTICAL	HORIZ.	VERTICAL	HORIZ.	VERTICAL	HORIZ.	VERTICAL	HORIZ.
LABORATORY	0.123	0.108	0.118	0.191				
TABLE MT.								
Test - 5					0.326	0.205	0.567	0.504
Test - 7						0.228		0.527
Test - 8						0.306		0.605
Test - 9					0.419	0.416	0.660	0.715
NASA - WFC								
Test - 1					0.269		0.510	
Test - 2					0.207		0.448	
Test - 3					0.269		0.510	
Test - 4					0.267		0.508	
Test - 5					0.266		0.516	
AVERAGE					0.289	0.289	0.531	0.588

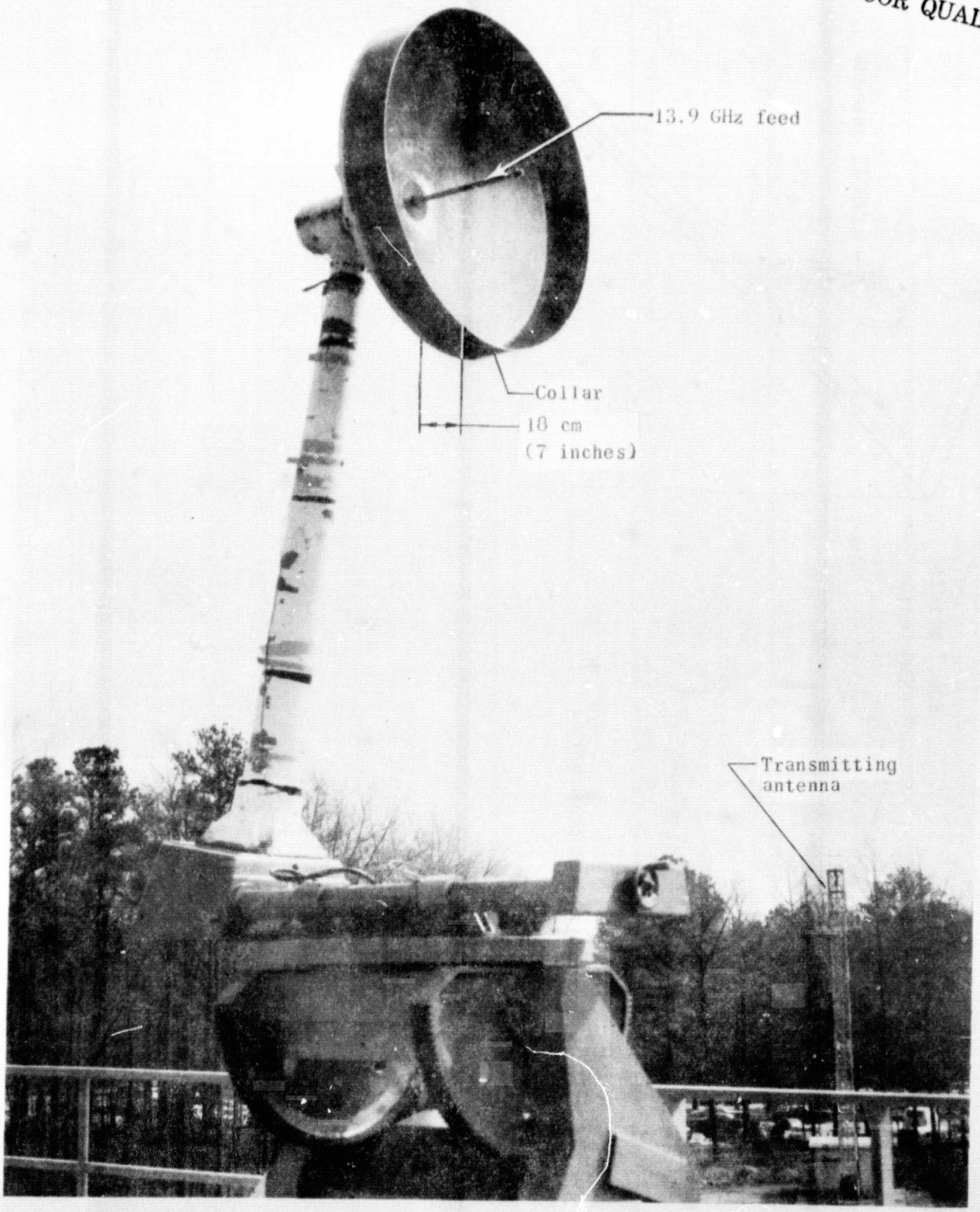

Figure 1 .-RADSCAT test antenna mounted on receiving pedestal.

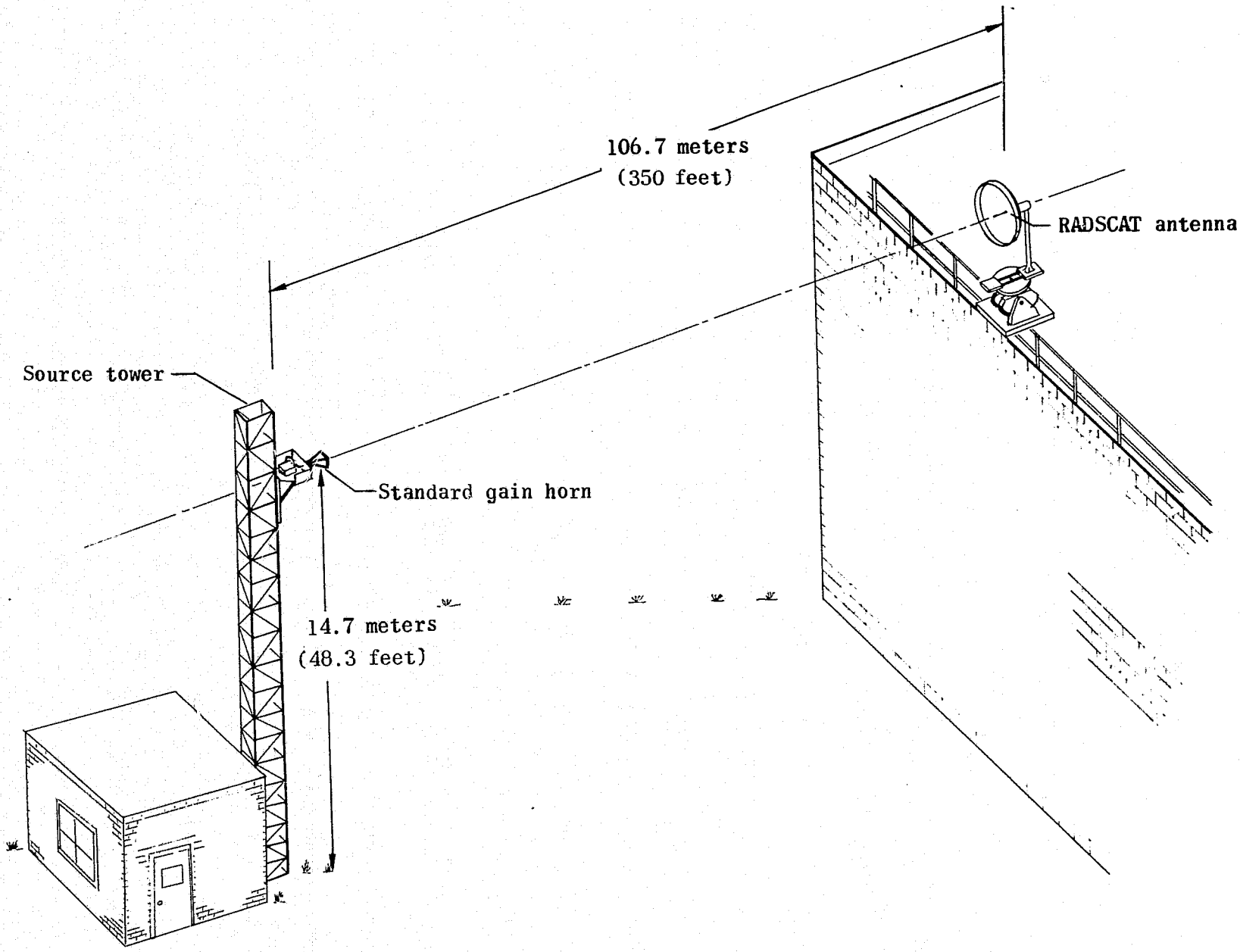

Figure 2 .-LaRC outdoor antenna test range.

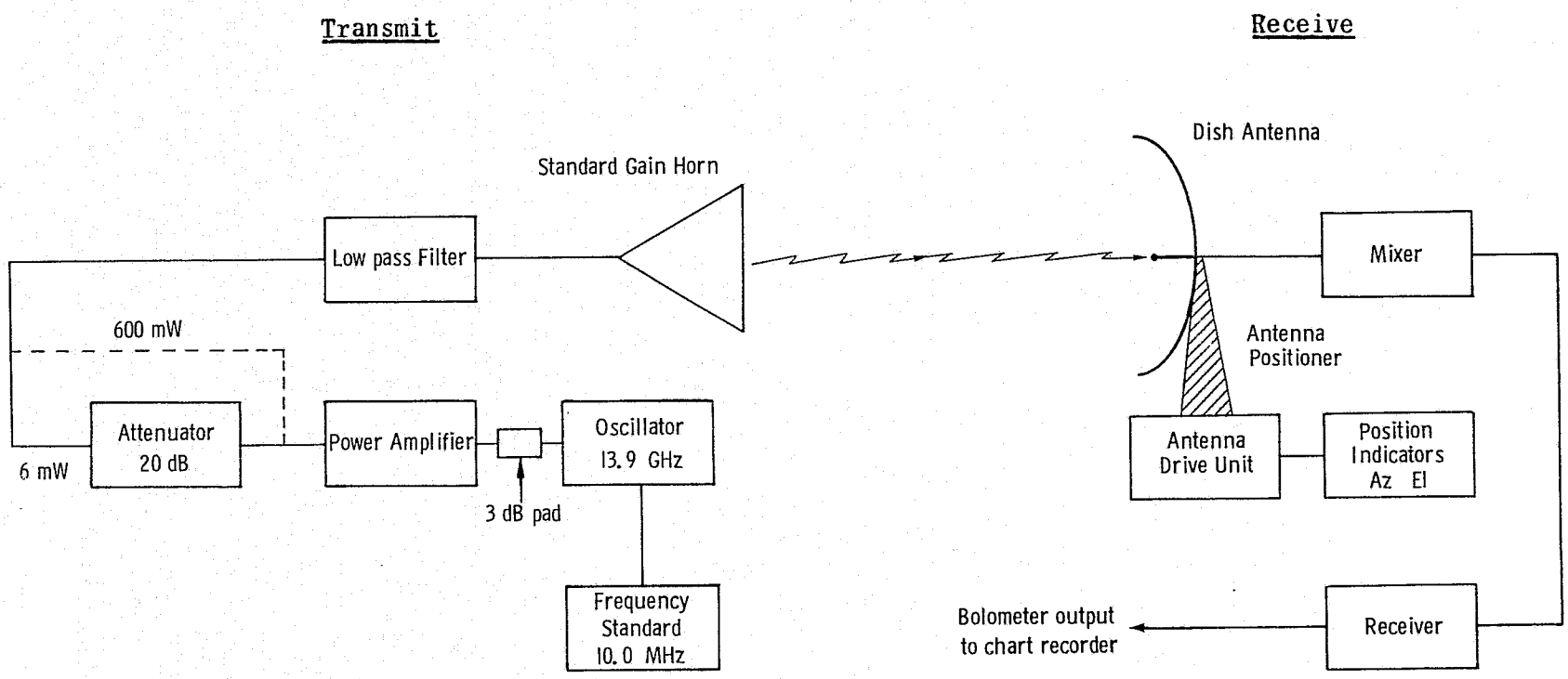

Figure 3 .- Transmit and receive electronics for RADSCAT antenna patterns.

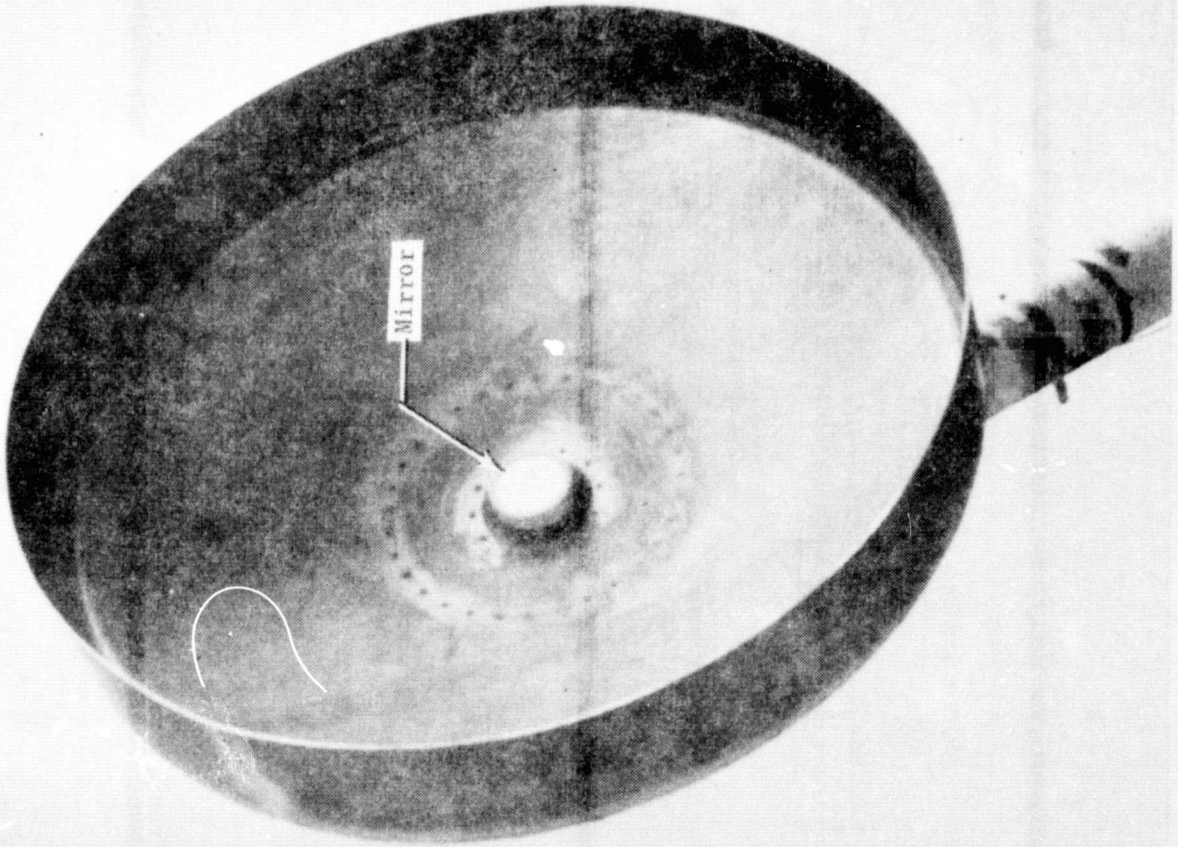

Figure 4.-RADSCAT antenna reflector with mirror mounted at feed point.

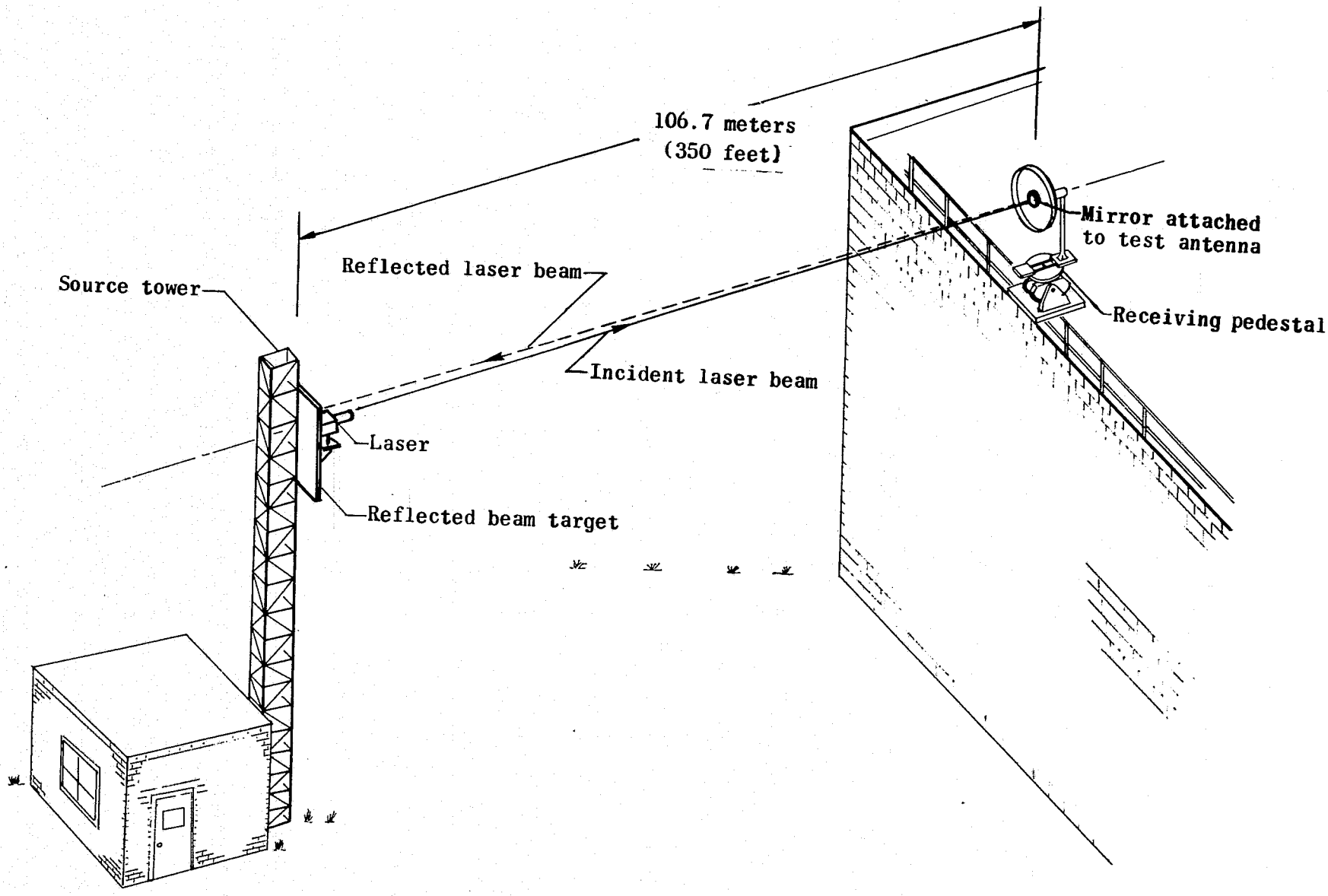
106.7 meters
(350 feet)
Mirror attached
to test antenna
Reflected laser beam
Source tower
Receiving pedestal
Incident laser beam
Laser
Reflected beam target

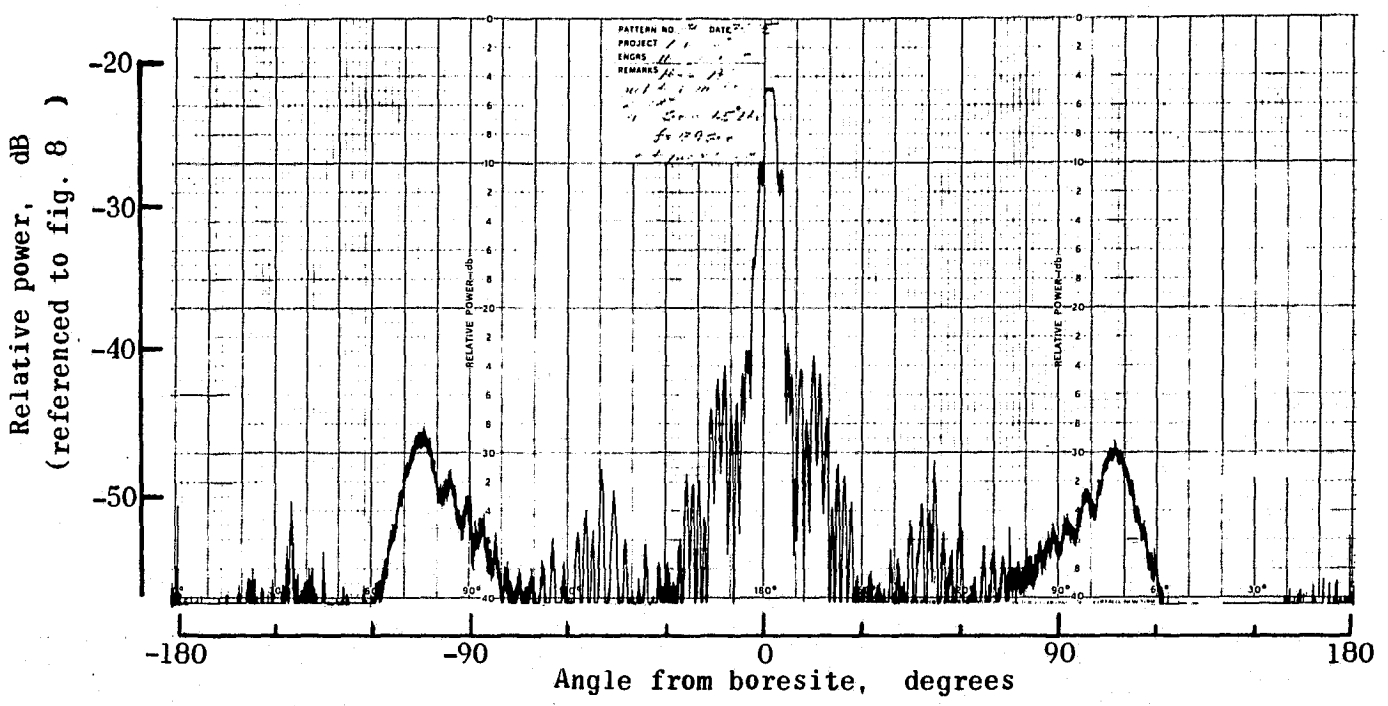

(a) No collar.

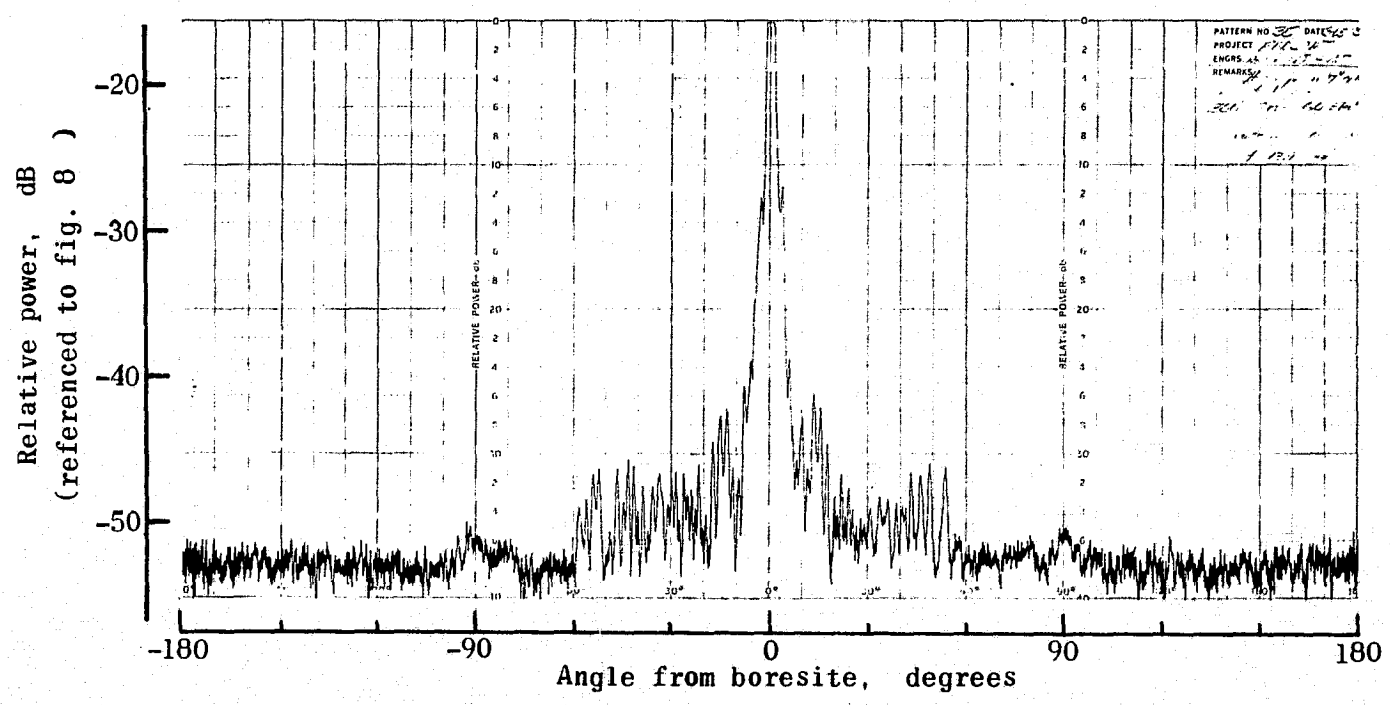

(b) Collar.

Figure 6.- Effects of collar on Horizontally-polarized antenna radiation patterns at 13.9 GHz using feed 1. Radiation power of 600 mW.

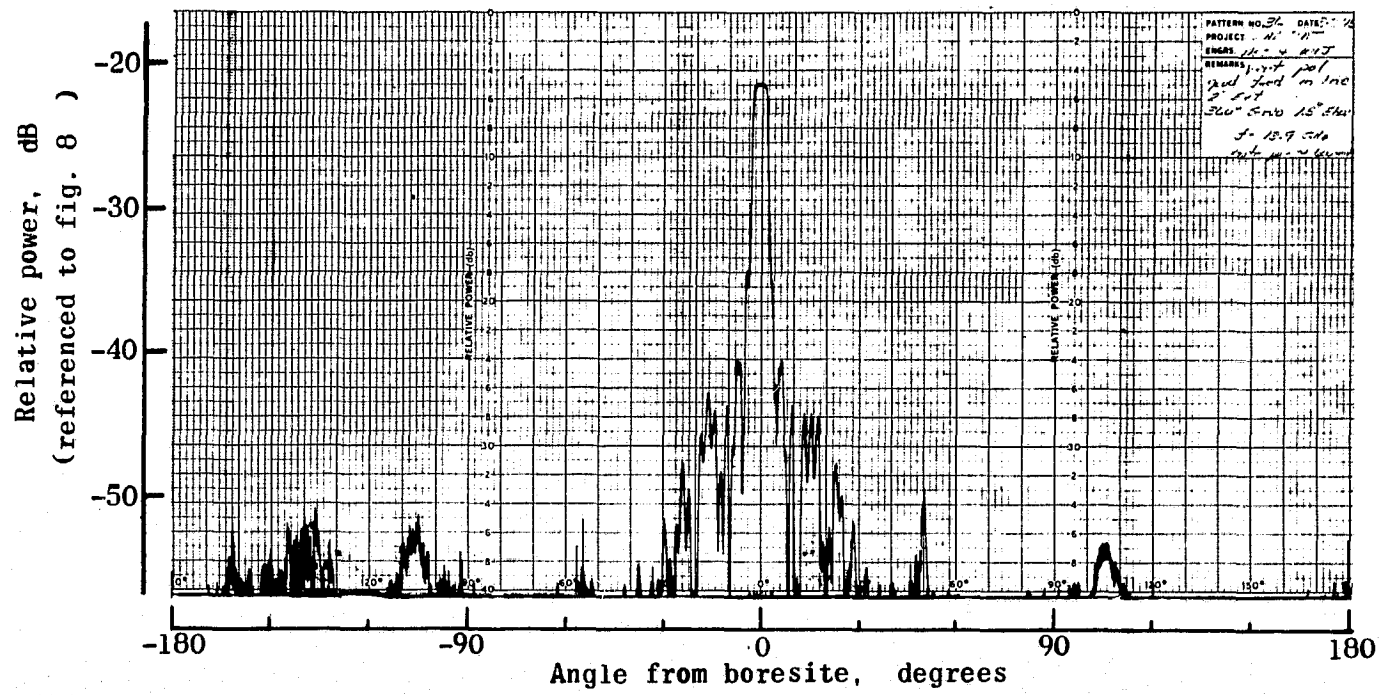

(a) No collar.

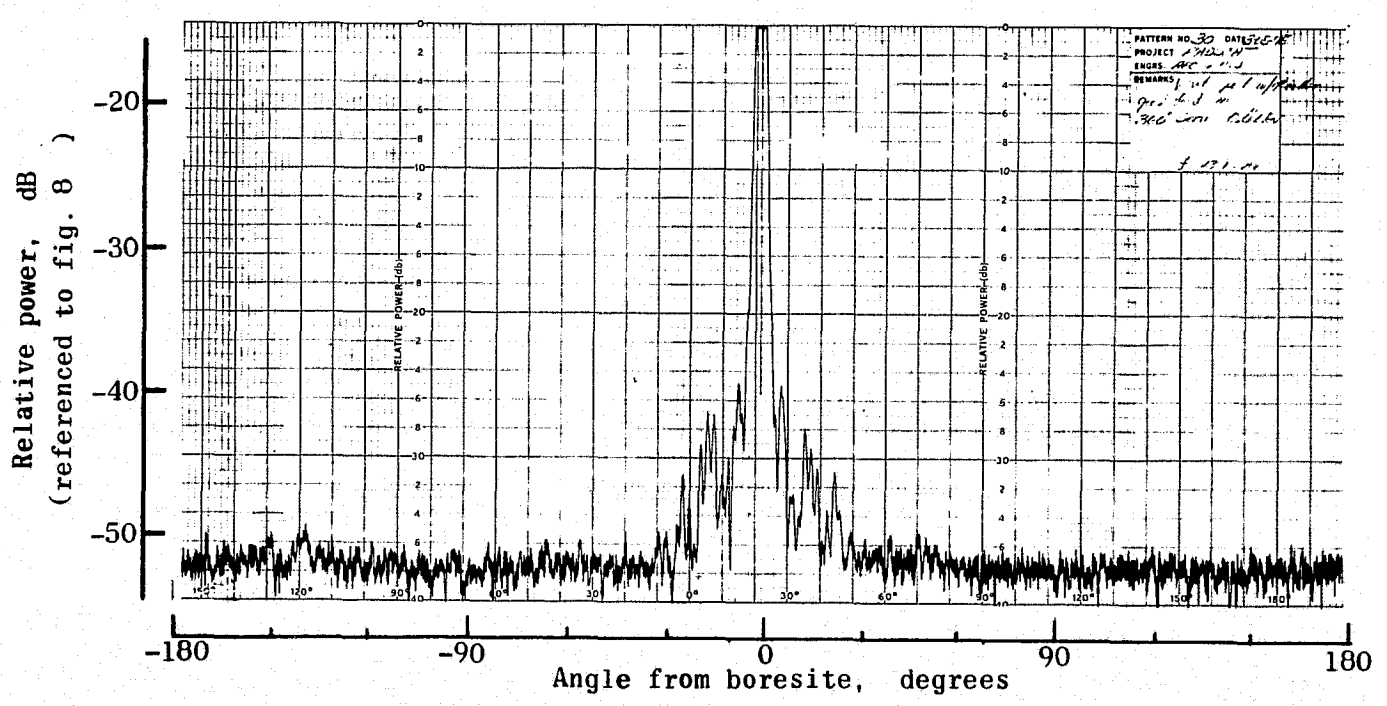

(b) Collar.

Figure 7. - Effects of collar on Vertically-polarized antenna radiation patterns at 13.9 GHz using feed 1. Radiation power of 600 mW.

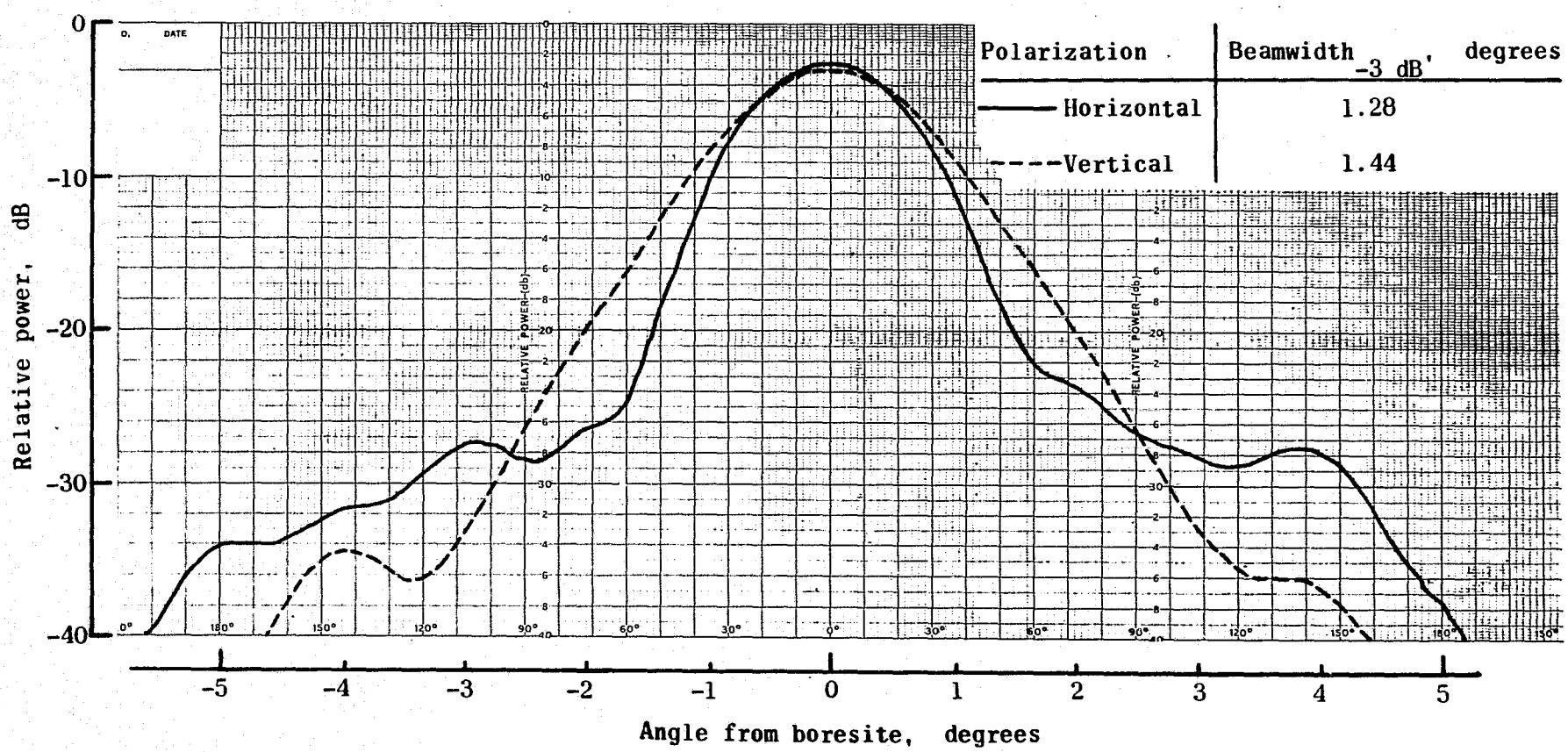

Figure 8 .- Principle beam radiation patterns without collar for Horizontal and Vertical polarizations at 13.9 GHz using feed 1. Radiation power of 6 mW.

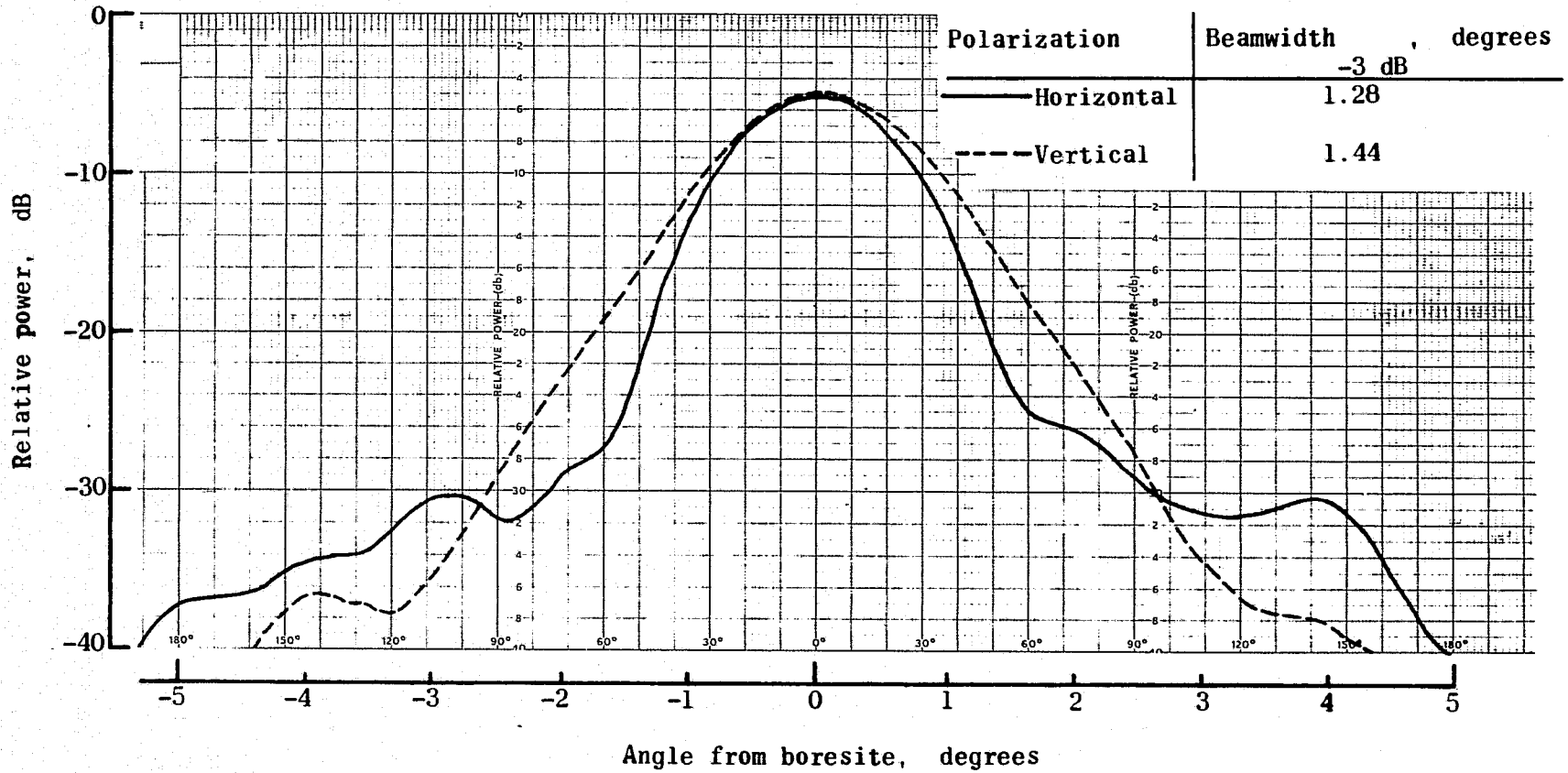

Figure 9 .- Principle beam radiation patterns without collar for Horizontal and Vertical polarizations at 13.9 GHz using feed 2. Radiation power of 6 mW.

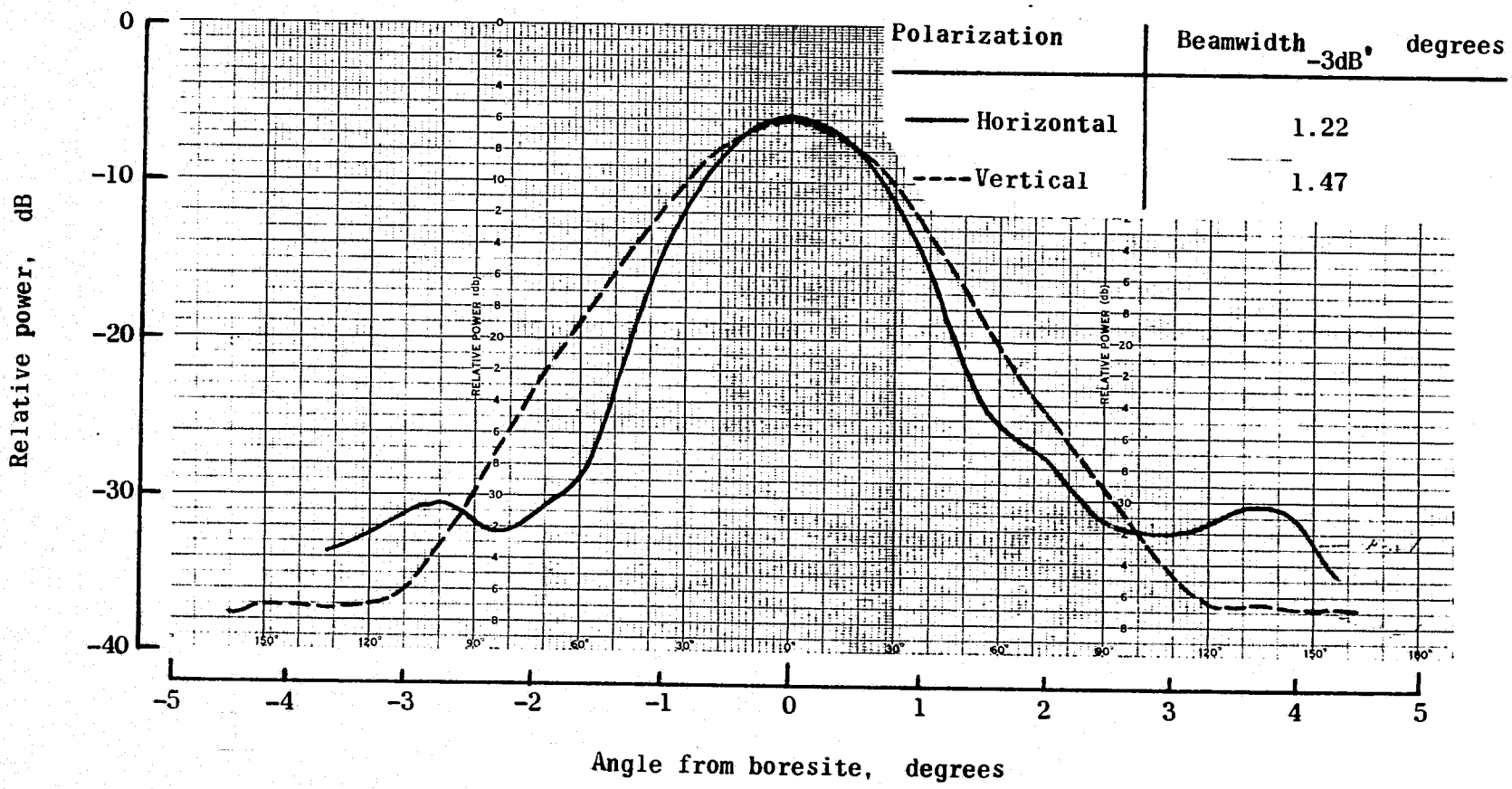

Figure 10.- Principle beam radiation patterns with collar for Horizontal and Vertical polarizations at 13.9 GHz using feed 1. Radiation power of 6 mW.

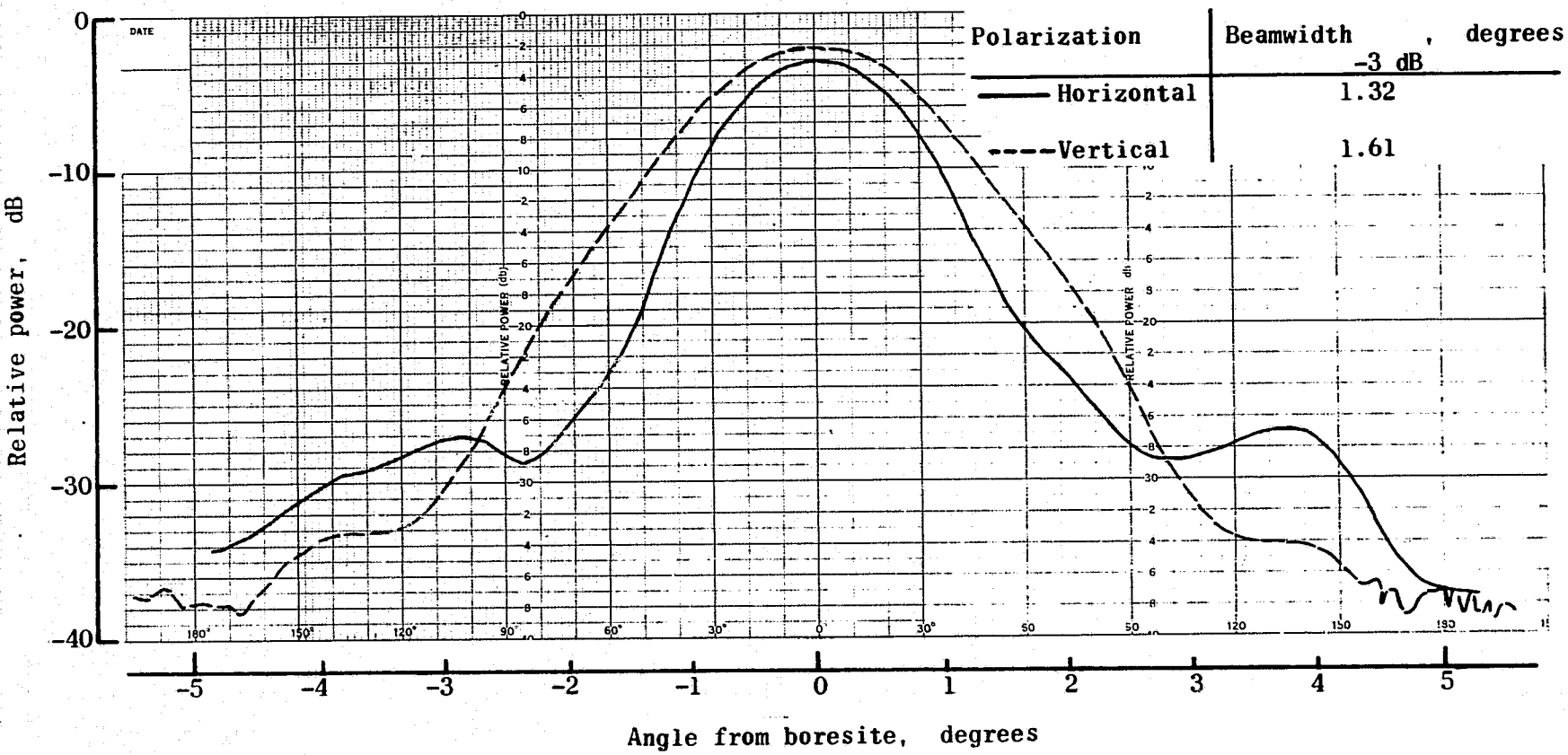

Figure 11.- Principle beam radiation patterns with collar for Horizontal and Vertical polarizations at 14.0 GHz using feed 1. Radiation power of 6 mW.

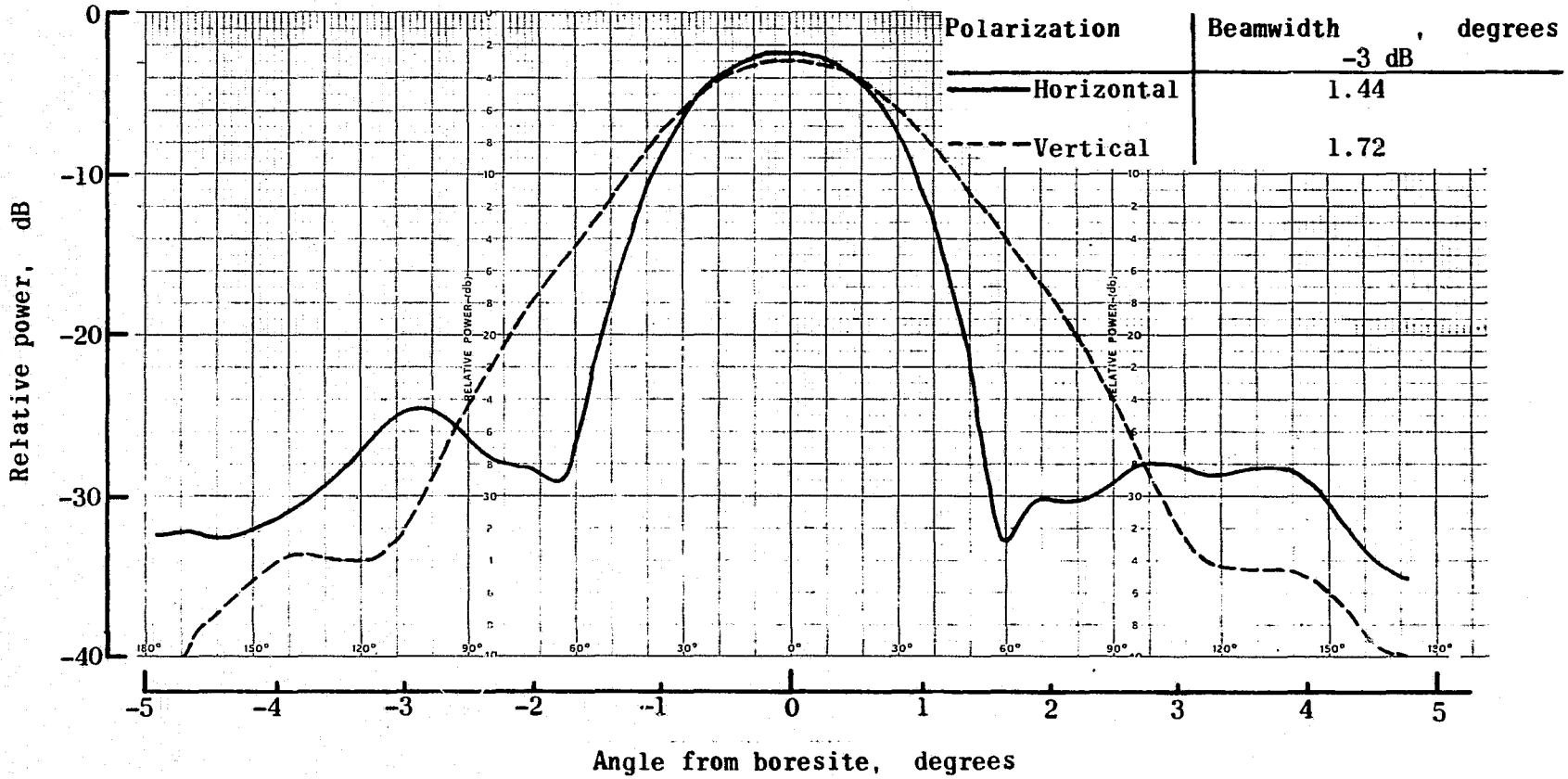

Figure 12.- Principle beam radiation patterns with collar for Horizontal and Vertical polarizations at 14.0 GHz using feed 2. Radiation power of 6 mW.

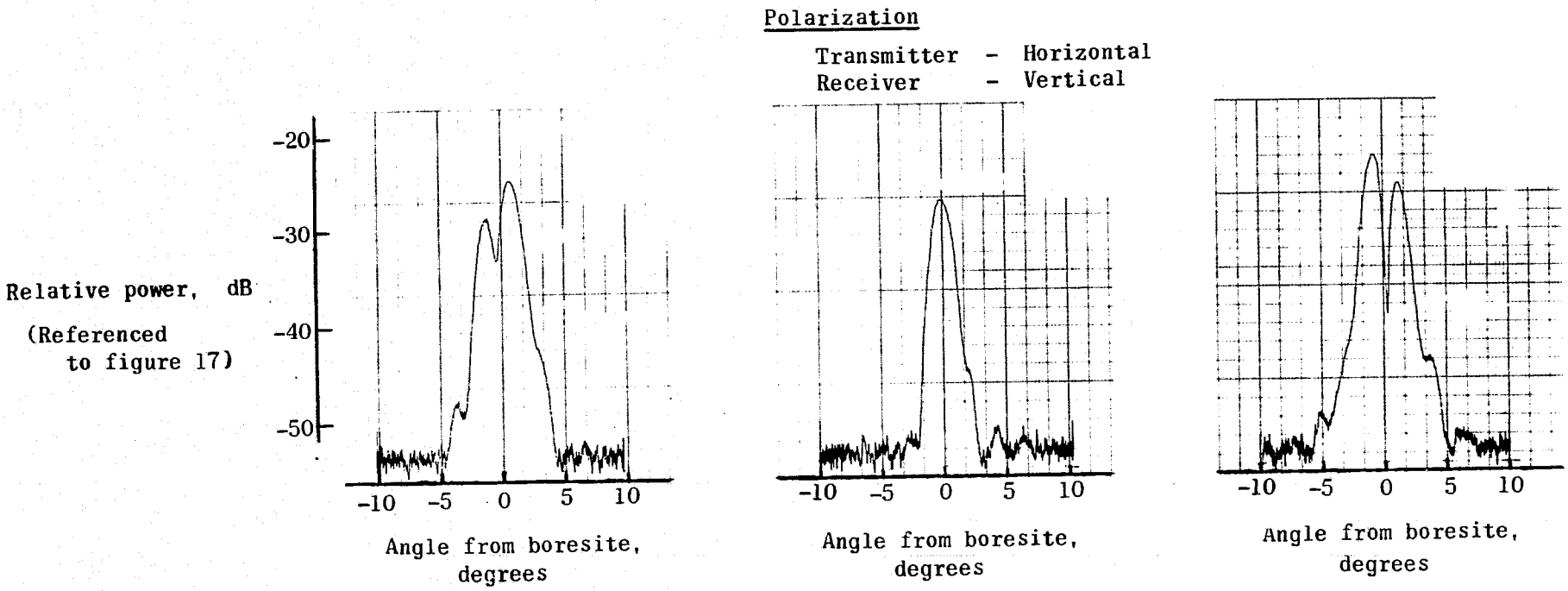

Figure 13.- Cross-polarized radiation patterns for RADSCAT antenna using feed 1 at a frequency of 13.9 GHz. Radiation power of 600 mW.

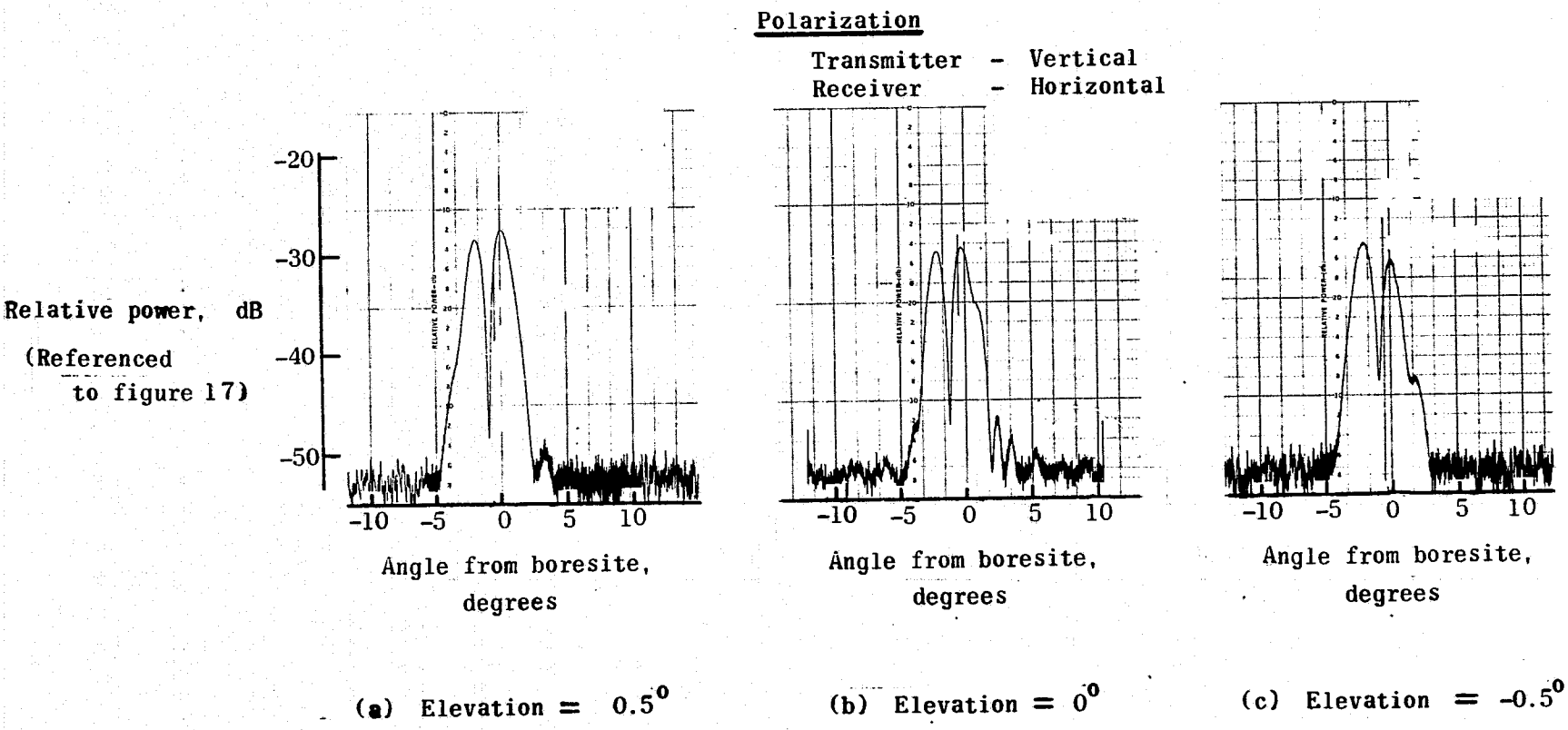

Figure 14.- Cross-polarized radiation patterns for RADSCAT antenna using feed 2 at a frequency of 13.9 GHz. Radiation power of 600 mW.

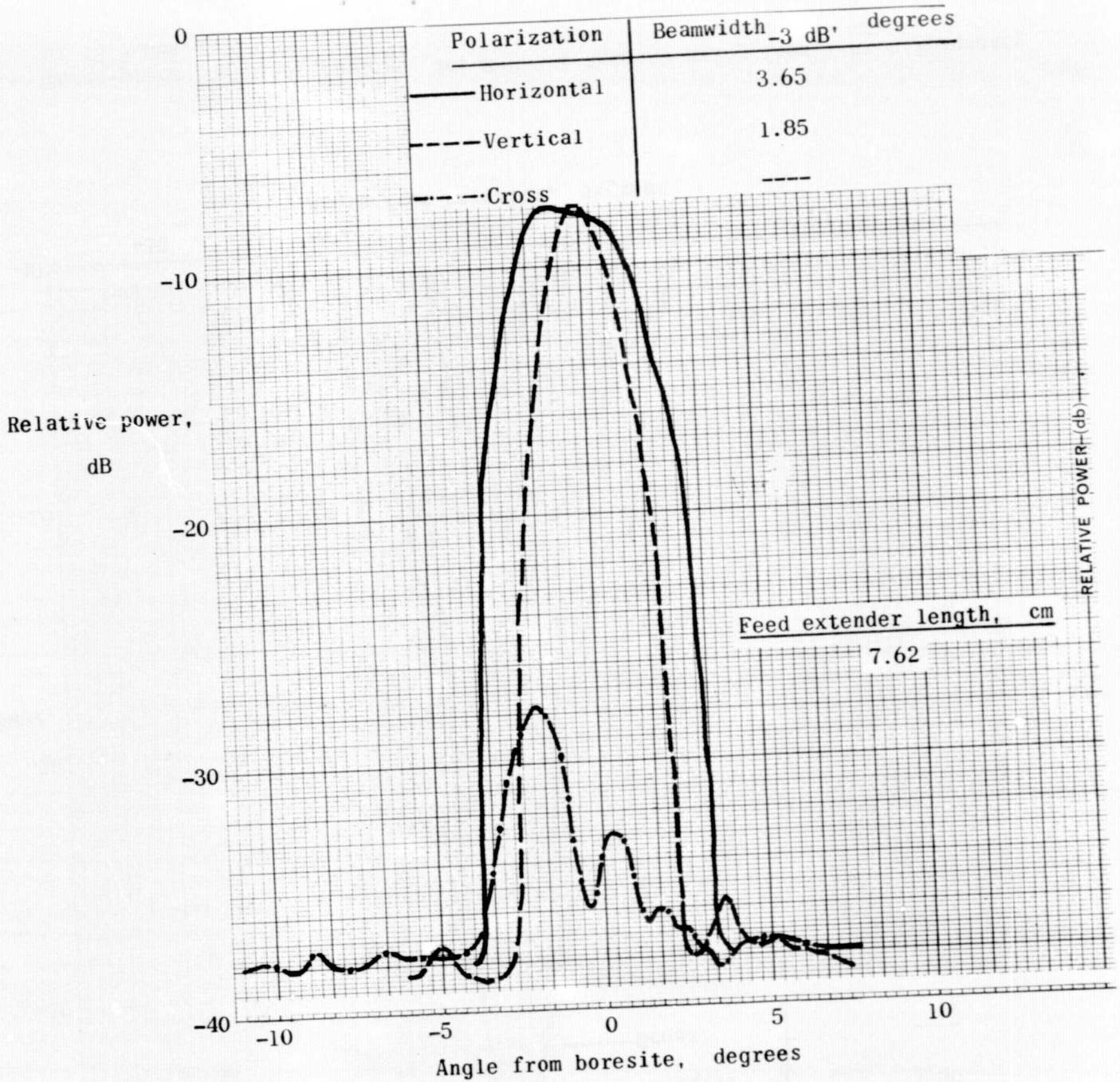

Figure 15.- Three-plane radiation patterns for RADSCAT antenna using feed 1 at a frequency of 14.0 GHz.

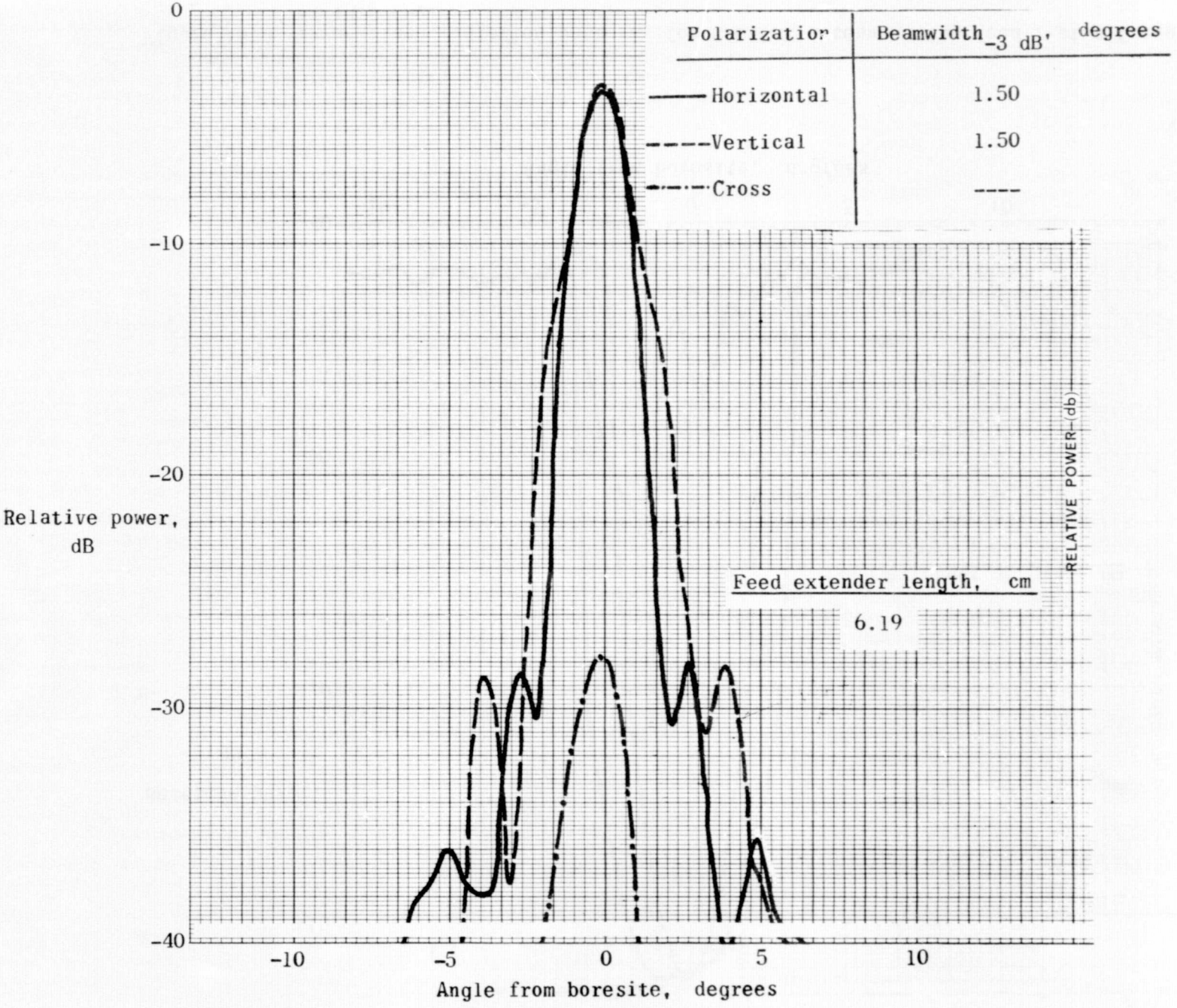

Figure 16.- Three-plane radiation patterns for RADSCAT antenna using feed 1 at a frequency of 13.9 GHz.

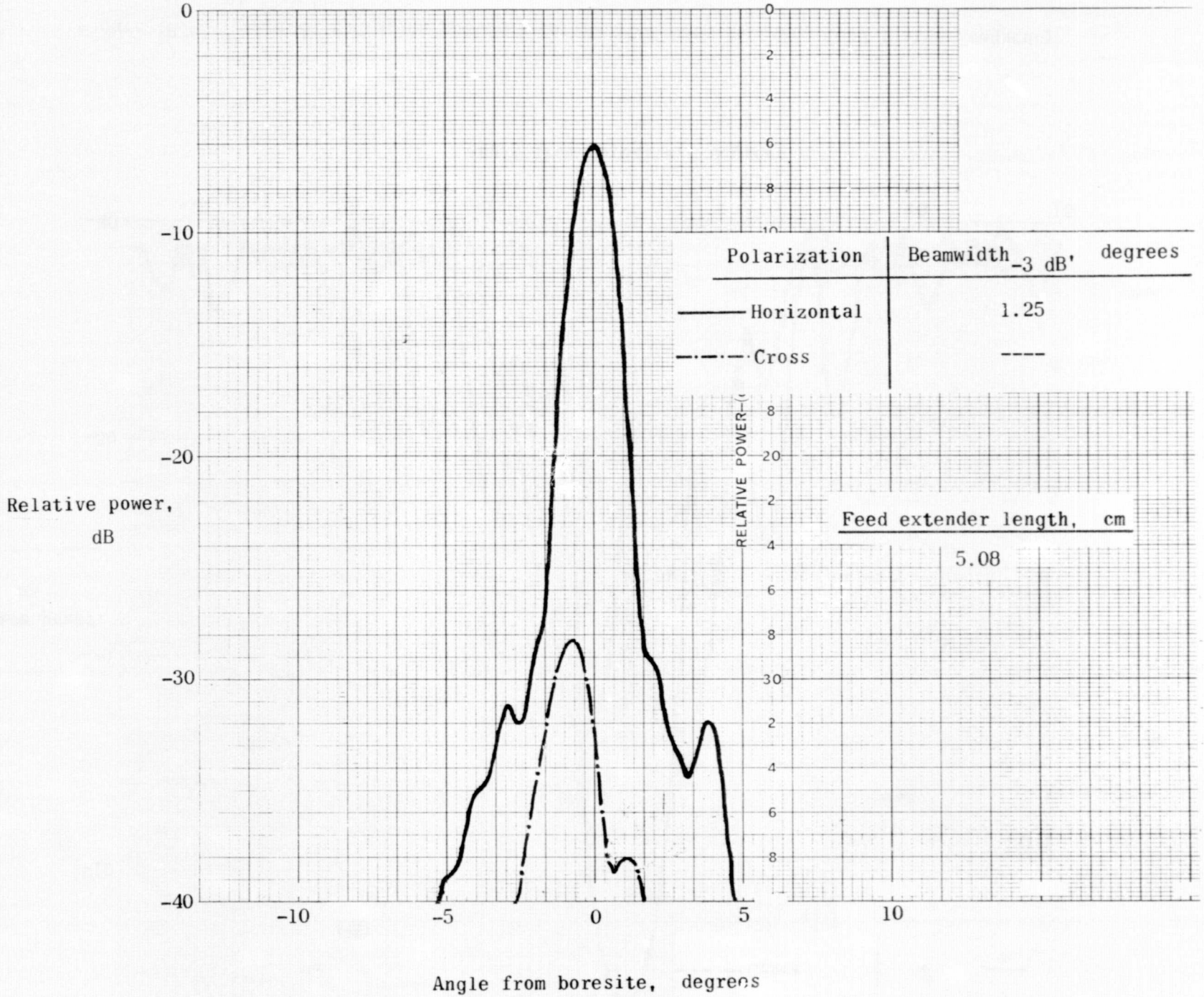

Figure 17.- Two-plane radiation patterns for RADSCAT antenna using feed 1 at a frequency of 13.9 GHz.

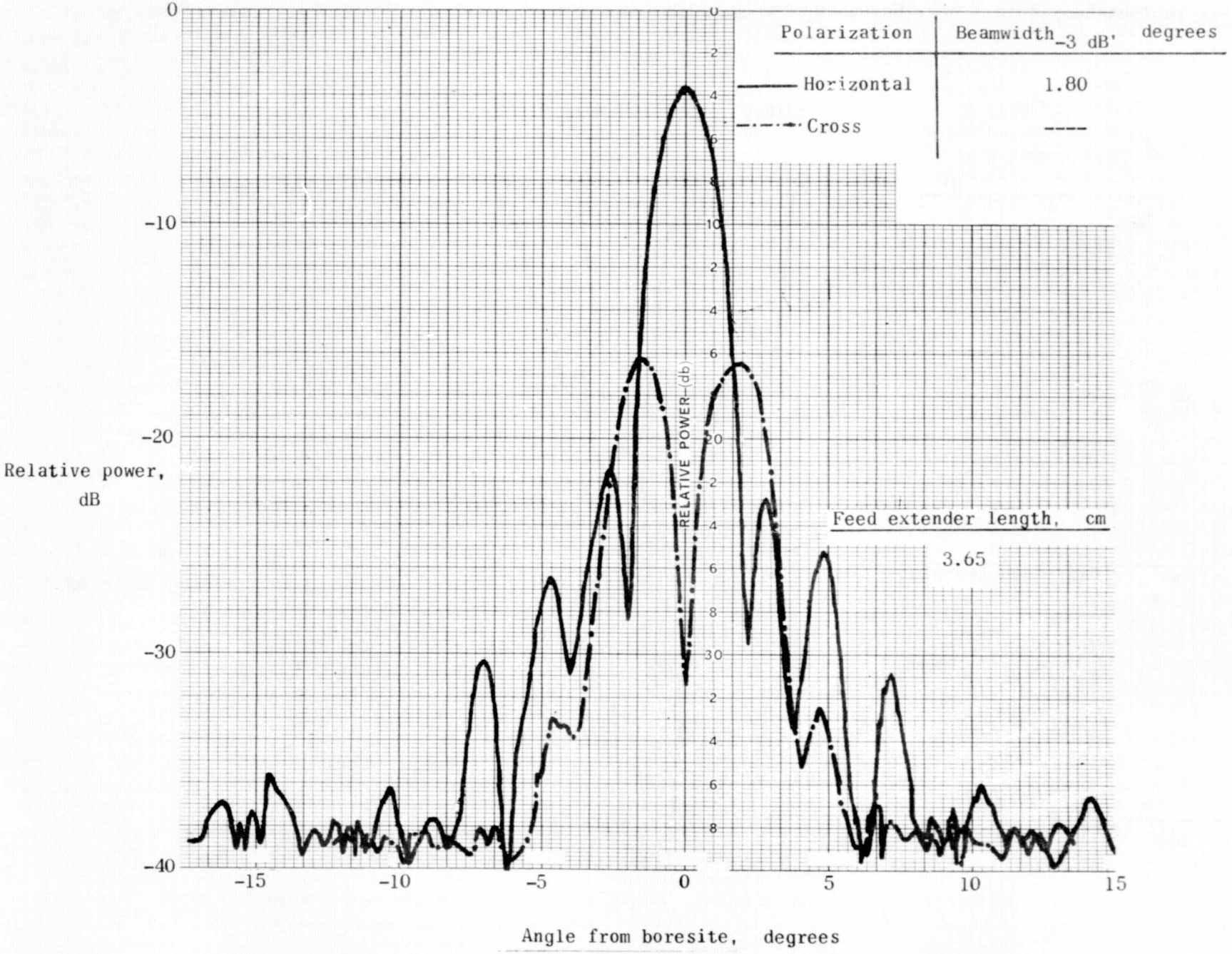

Figure 18.- Two-plane radiation patterns for RADSCAT antenna using feed 1 at a frequency of 13.9 GHz.

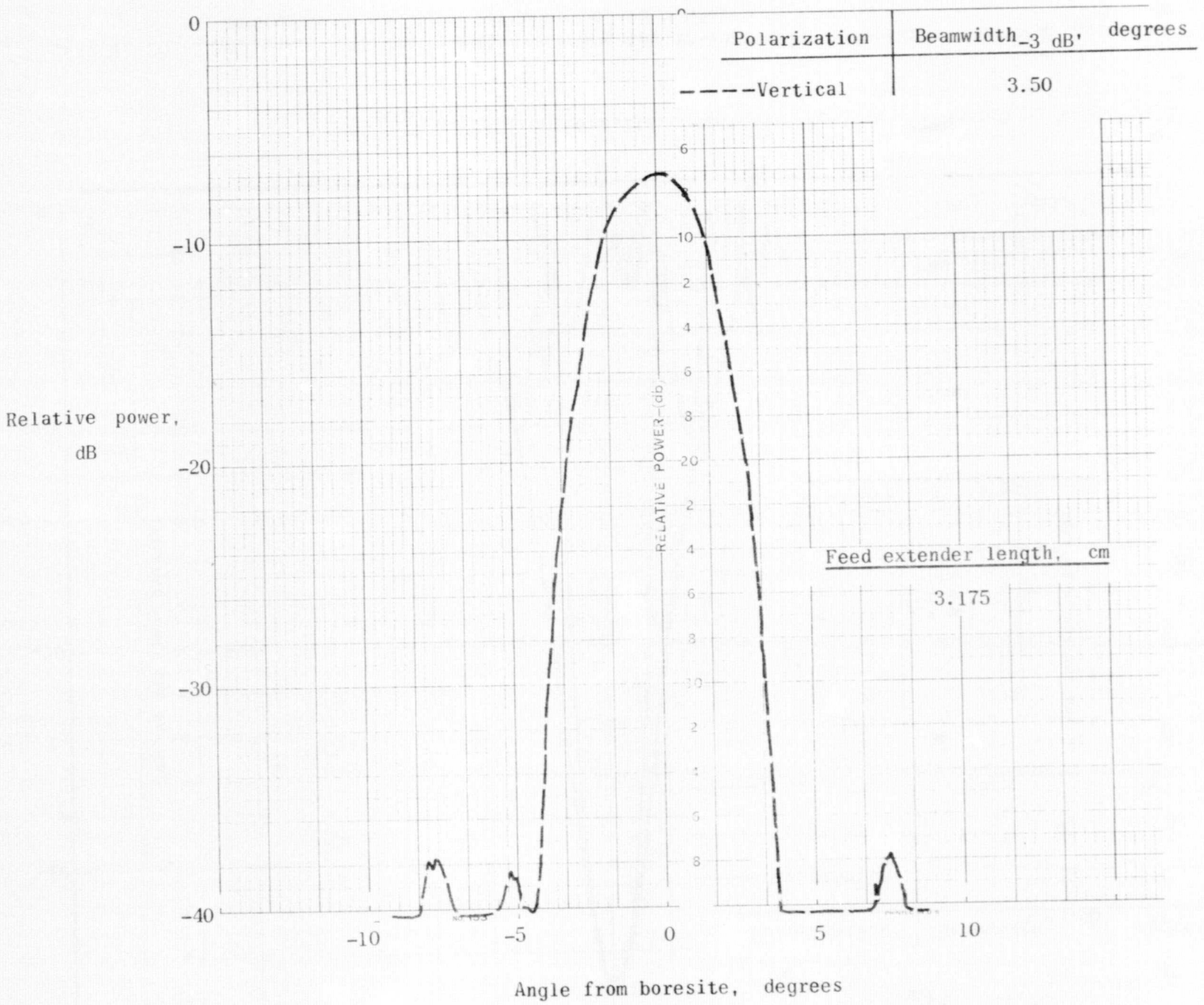

Figure 19.- Vertically polarized radiation pattern of RADSCAT antenna using feed 1 at a frequency of 13.9 GHz.

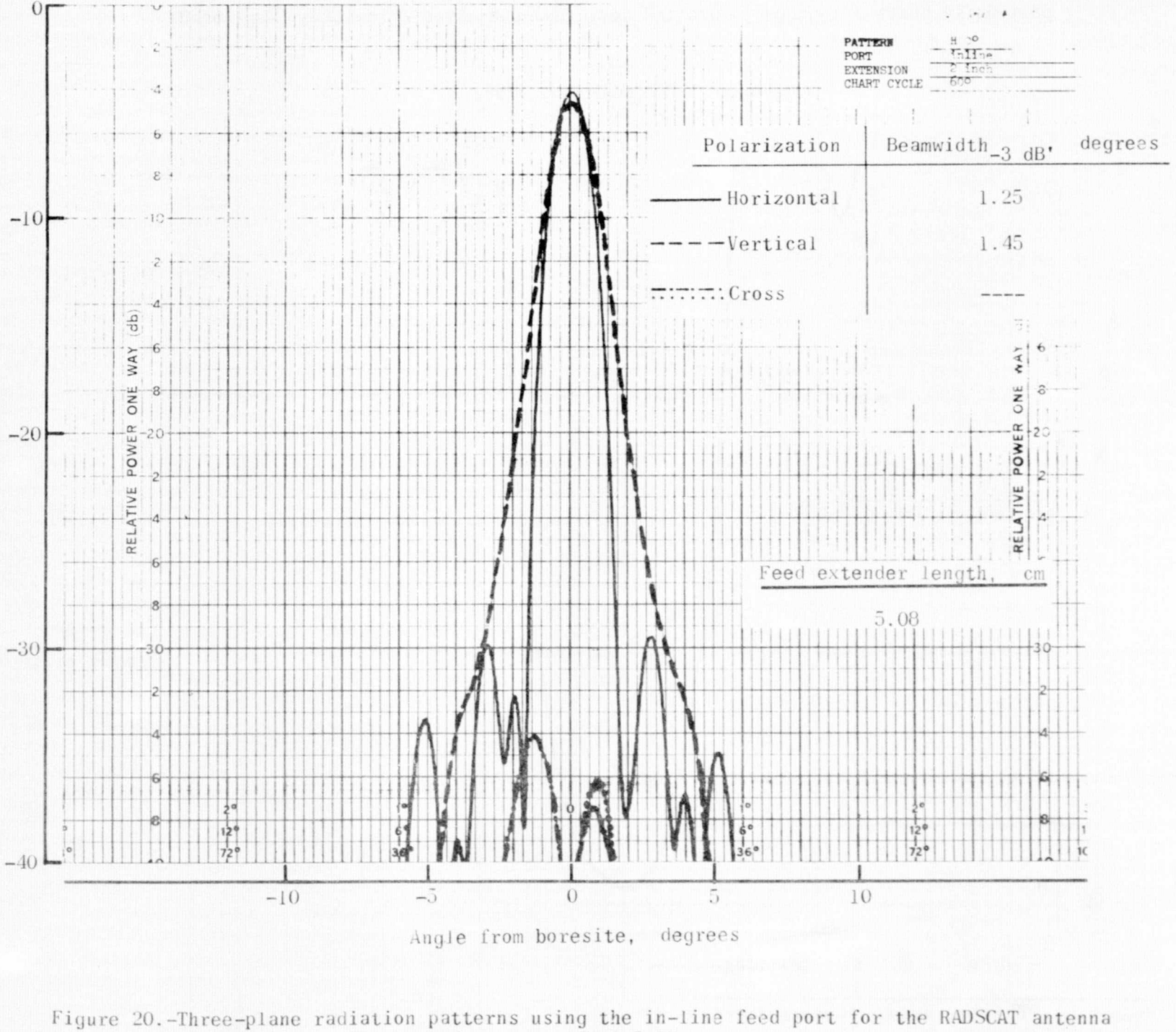

Figure 20.-Three-plane radiation patterns using the in-line feed port for the RADSCAT antenna as measured by JSC at a frequency of 13.9 GHz.

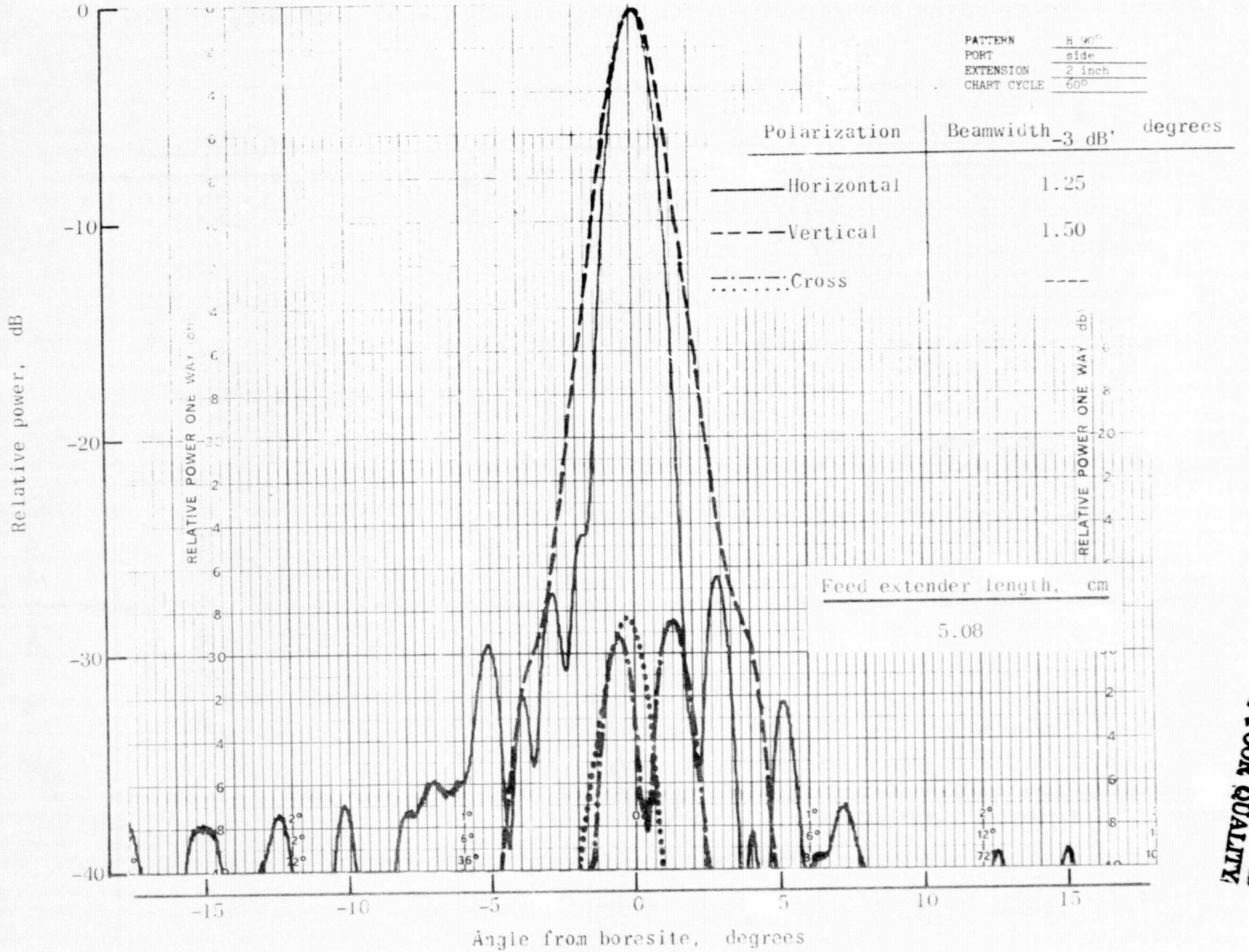

Figure 21.-Three-plane radiation patterns using the side feed port for the RADSCAT antenna as measured by JSC at a frequency of 13.9 GHz.

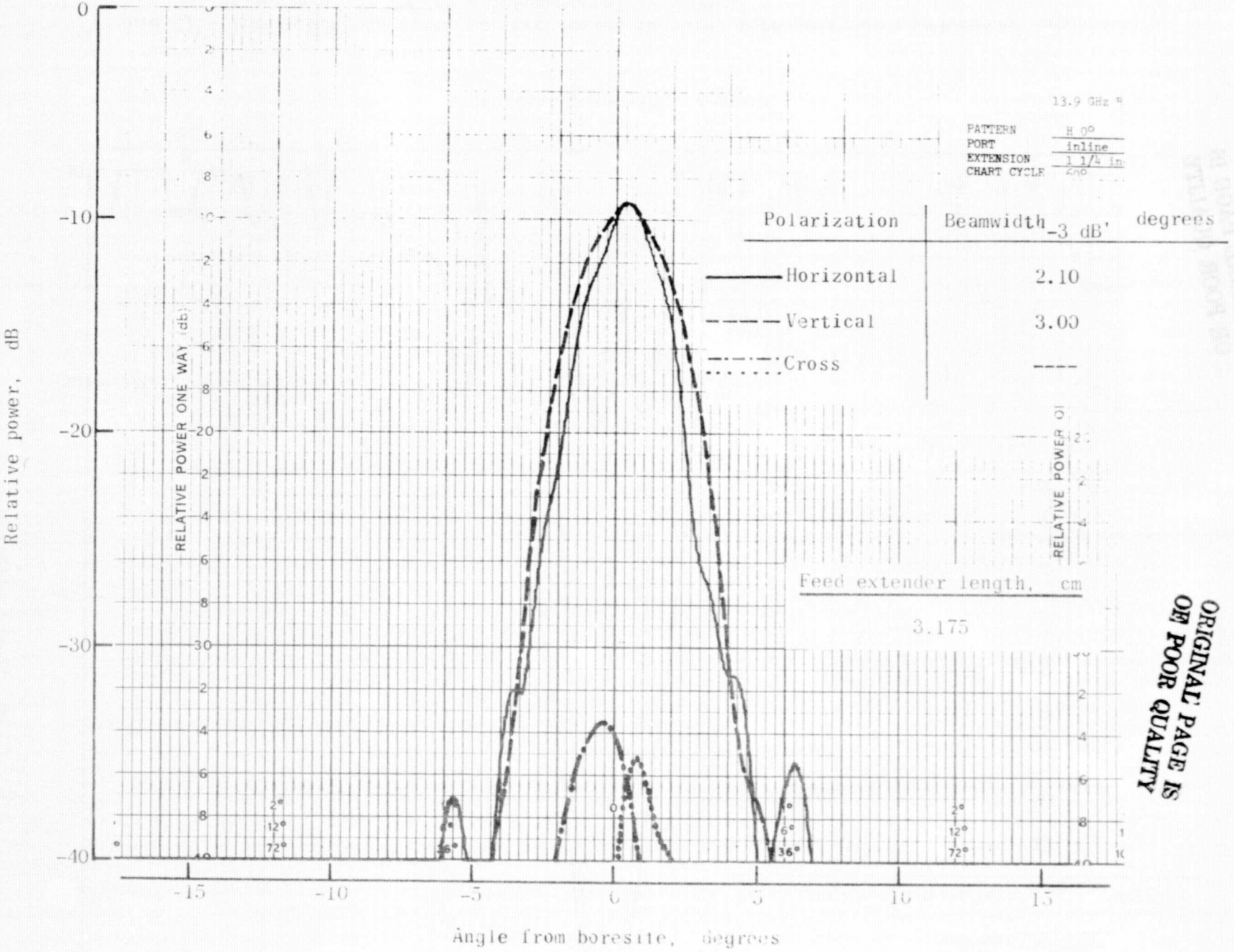

Figure 22.-Three-plane radiation patterns using the in-line feed port for the RADSCAT antenna as measured by JSC at a frequency of 13.9 GHz.

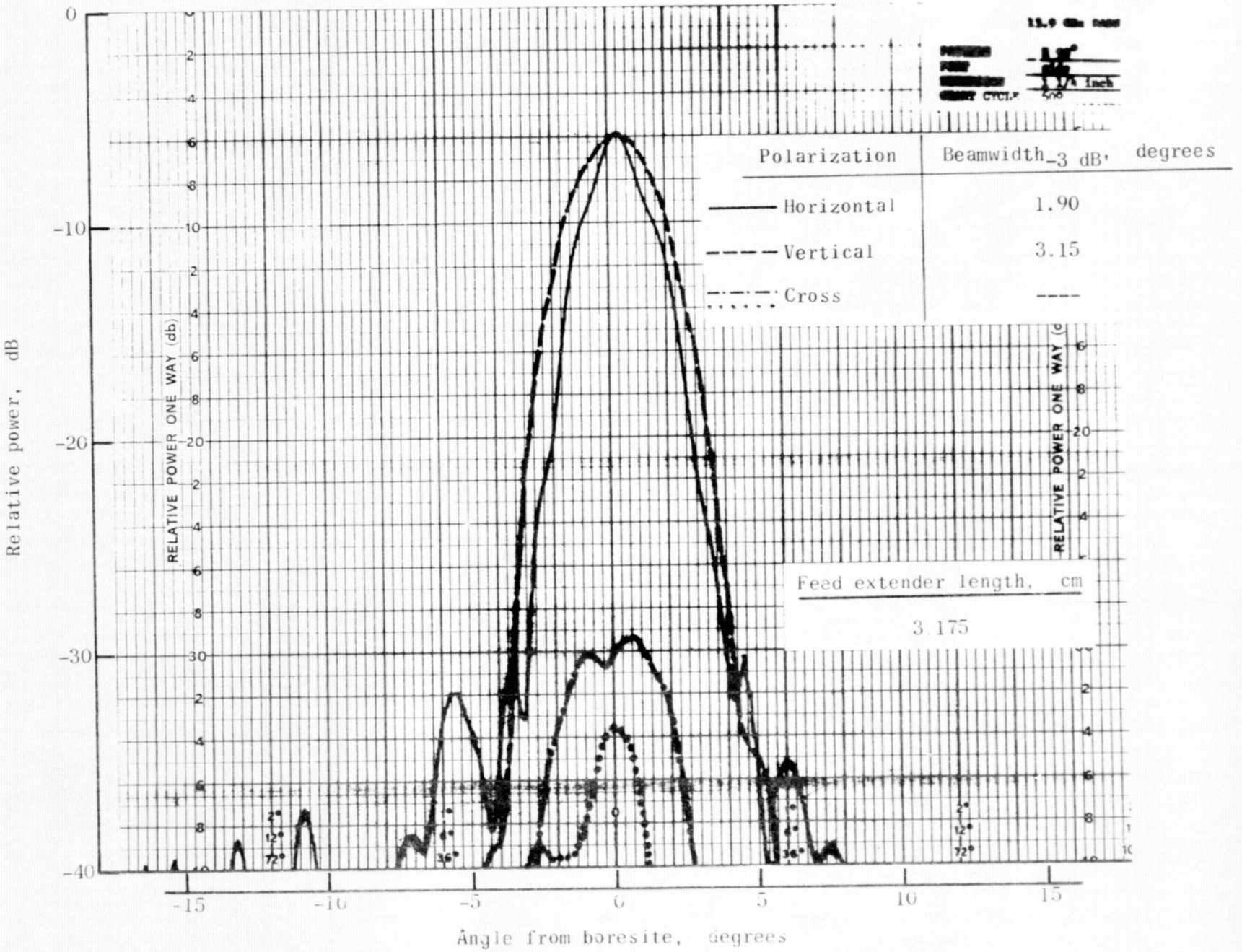

Figure 23.-Three-plane radiation patterns using the side feed port for the RADSCAT antenna as measured by JSC at a frequency of 13.9 GHz.

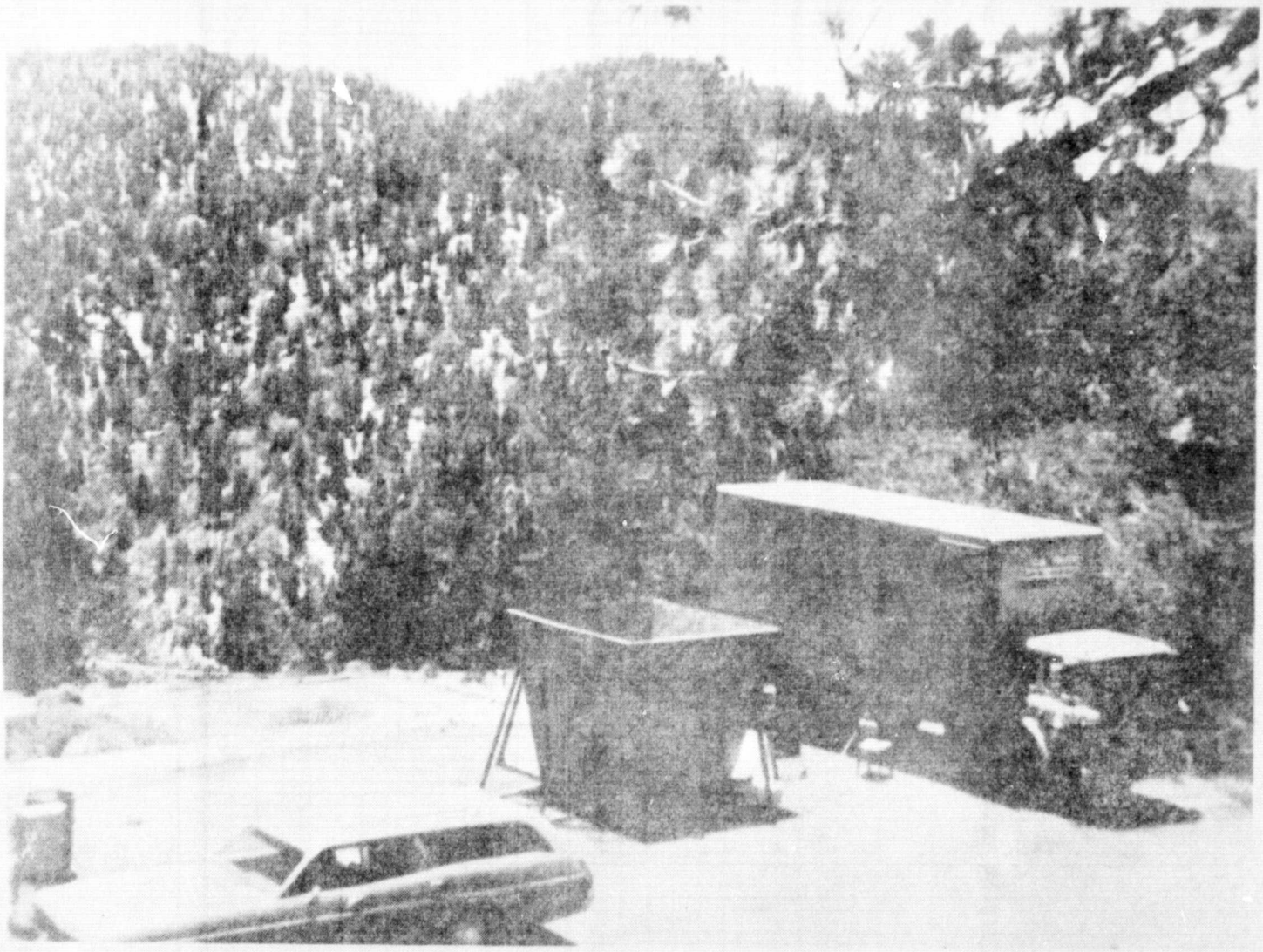

Figure 24.- Antenna loss measurements.

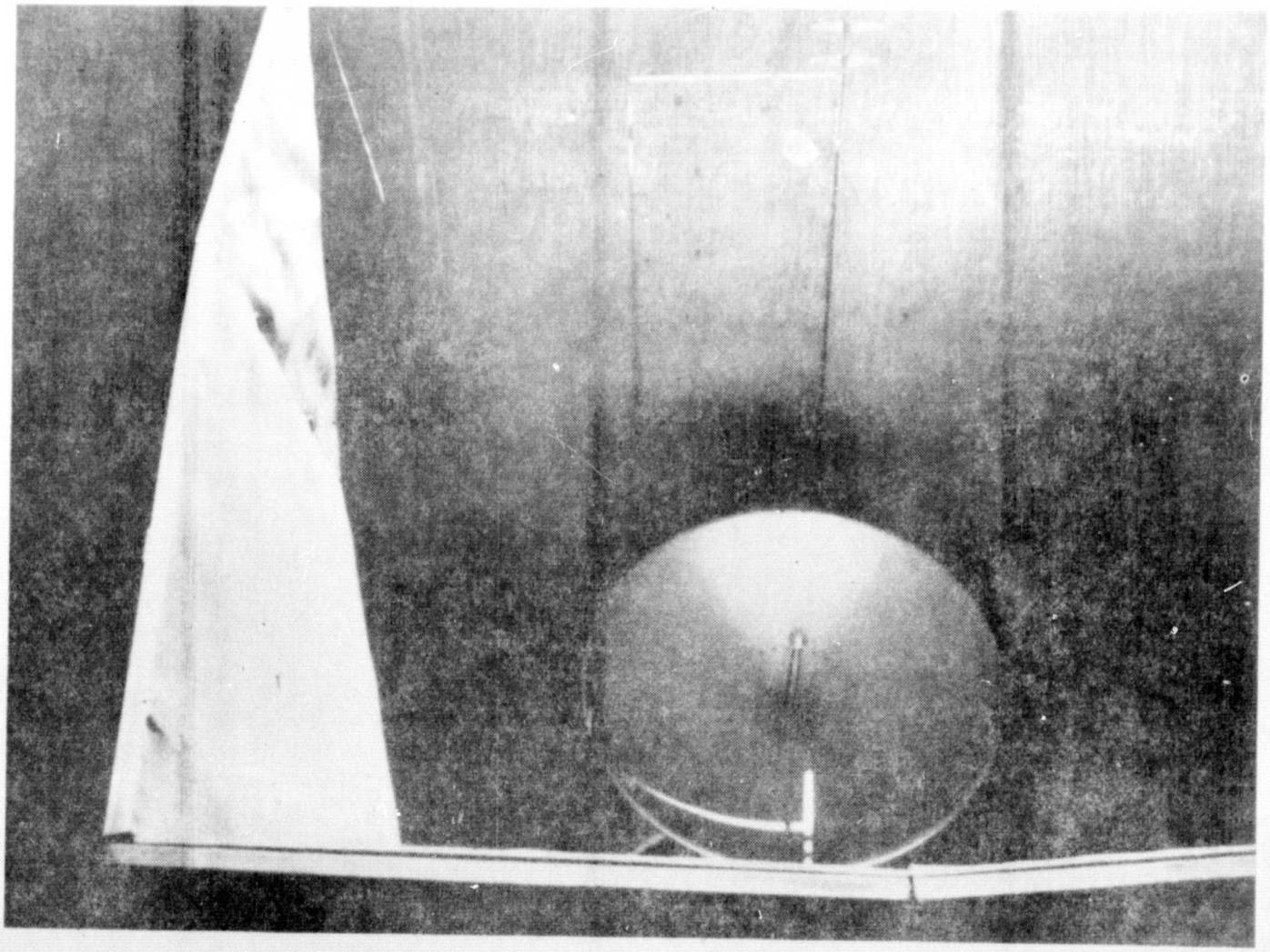

Figure 25.- RADSCAT antenna in reflector.

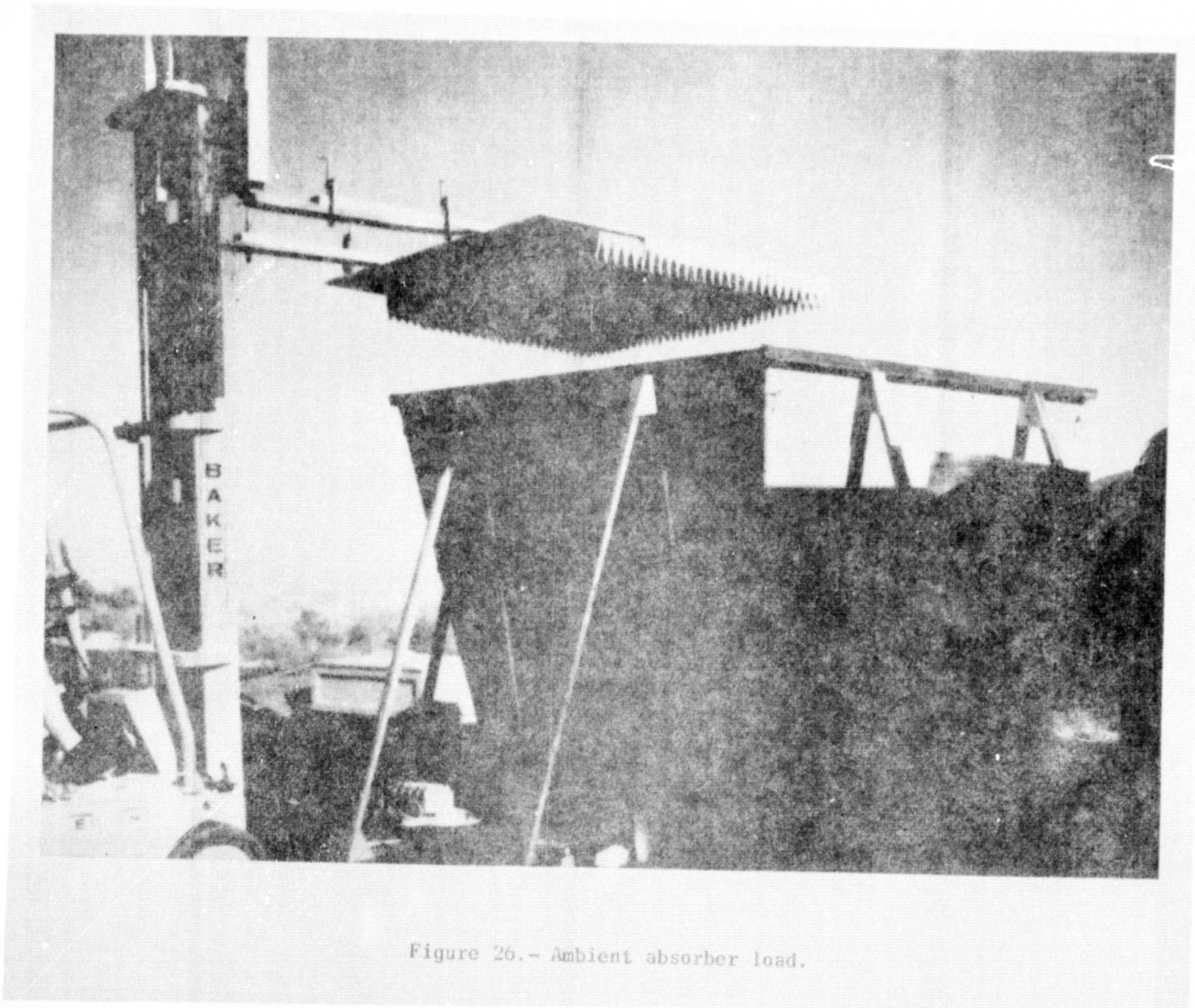

Figure 26.- Ambient absorber load.

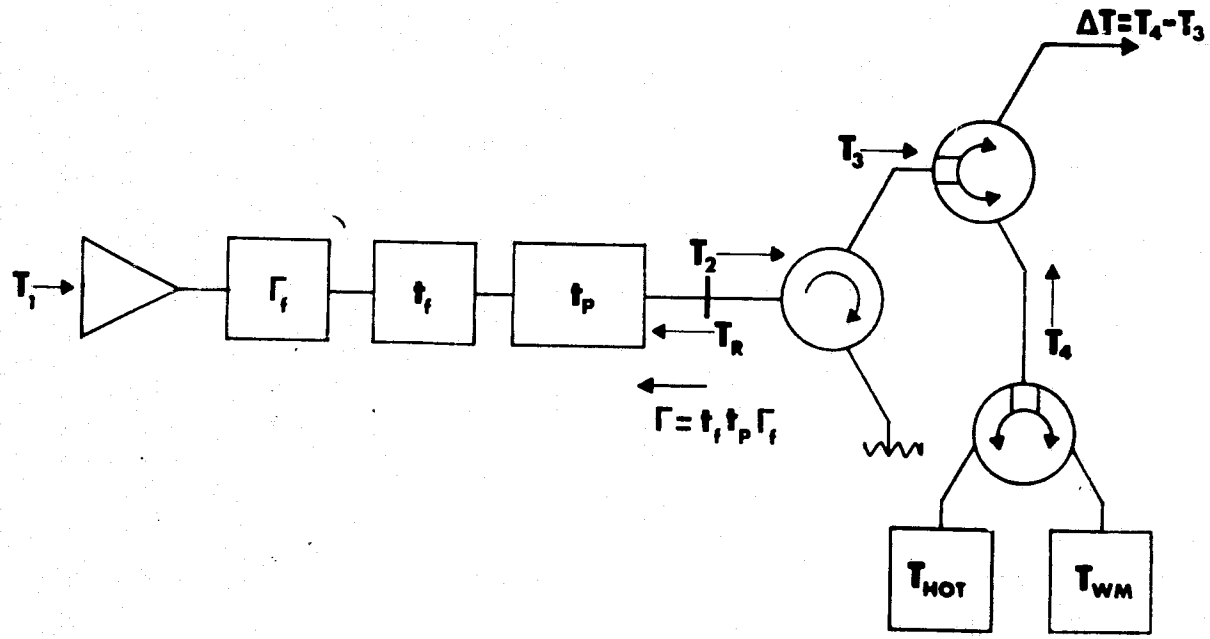

$$T_2 = \left(1 - \frac{\Gamma^2}{t_f^2 t_p^2}\right) T_1 t_f t_p + (1 - t_f) T_f t_p + (1 - t_p) T_p + \Gamma^2 T_R$$

Figure 27.- Transmission-line model of radiometer front end.

1 Report No.	2. Government Accession No.	3. Recipient's Catalog No.
NASA TM X-72844		

4. Title and Subtitle	5. Report Date
Measurements of AAFE RADSCAT Antenna Characteristics	June 1977
	6. Performing Organization Code
7. Author(s)	8. Performing Organization Report No.
Aubrey E. Cross, W. Linwood Jones, and Alfred L. Jones	
	10. Work Unit No.
9. Performing Organization Name and Address	11. Contract or Grant No.
NASA Langley Research Center Hampton, Virginia 23665	
	13. Type of Report and Period Covered
12. Sponsoring Agency Name and Address	NASA Technical Memorandum
National Aeronautics & Space Administration Washington, D. C. , 20546	14. Sponsoring Agency Code

15. Supplementary Notes

16. Abstract

Antenna characteristics (active and passive) for a modified AAFE-RADSCAT parabolic dish antenna are documented for a variety of antenna configurations. The modified antenna was a replacement for the original unit which was damaged in January 1975. Pattern measurements made at Langley Research Center and Johnson Space Center are presented, with an analysis of the results. Antenna loss measurements are also presented and summarized.

17. Key Words (Suggested by Author(s))	18. Distribution Statement
AAFE-RADSCAT Antennas	UNCLASSIFIED-UNLIMITED

19. Security Classif. (of this report)	20. Security Classif. (of this page)	21. No. of Pages	22. Price*
UNCLASSIFIED	UNCLASSIFIED	40	$4.00

*For sale by the National Technical Information Service, Springfield, Virginia 22161